TKK Radio Science and Engineering Publications
Espoo, July 2009 REPORT R8

MICROWAVE TRANSMISSION-LINE NETWORKS FOR BACKWARD-WAVE MEDIA AND REDUCTION OF SCATTERING

Thesis for the degree of Doctor of Science in Technology

Pekka Alitalo

Dissertation for the degree of Doctor of Science in Technology to be presented with due permission of the Faculty of Electronics, Communications and Automation, for public examination and debate in Auditorium S4 at Helsinki University of Technology (Espoo, Finland) on the 7th of August, 2009, at 12 o'clock noon.

Helsinki University of Technology
Faculty of Electronics, Communications, and Automation
Department of Radio Science and Engineering

Cover:
Simulated electric field distributions in a rectangular waveguide (left), waveguide with an array of metal cylinders creating a short-circuit in the waveguide (center), and waveguide with the array cloaked by a transmission-line structure (right).

Distribution:
Helsinki University of Technology
Department of Radio Science and Engineering
P.O. Box 3000
FI-02015 TKK
Tel. +358 9 451 2261
Fax +358 9 451 2267
E-mail ari.sihvola@tkk.fi

ISBN 978-951-22-9986-7 (paper)
ISBN 978-951-22-9987-4 (electronic)
ISSN 1797-4364 (paper)
ISSN 1797-8467 (electronic)

Picaset Oy, Helsinki 2009

ABSTRACT OF DOCTORAL DISSERTATION	HELSINKI UNIVERSITY OF TECHNOLOGY P. O. BOX 1000, FI-02015 TKK http://www.tkk.fi

Author Pekka Alitalo

Name of the dissertation

Microwave Transmission-Line Networks for Backward-Wave Media and Reduction of Scattering

Manuscript submitted March 20, 2009	Manuscript revised July 1, 2009
Date of the defence August 7, 2009	
☐ Monograph	☒ Article dissertation (summary + original articles)

Faculty	Faculty of Electronics, Communications and Automation
Department	Department of Radio Science and Engineering
Field of research	Radio Engineering
Opponent(s)	Professor Christophe Caloz, École Polytechnique Montréal
Supervisor	Professor Sergei Tretyakov
Instructor	Professor Sergei Tretyakov

Abstract

This thesis investigates the use of transmission-line networks in various structures and devices that exhibit exotic response to impinging electromagnetic radiation. The main topics that are studied are media supporting backward-wave propagation, structures capable of electromagnetic cloaking, and a novel way of implementing microwave lenses with volumetric transmission-line networks.

Backward-wave media support propagation of electromagnetic waves for which the phase advances in the direction opposite to the energy propagation. Such media can be very useful due to certain exotic phenomena, for example, negative refraction and resonant enhancement of evanescent fields, that enable imaging with sub-wavelength resolution. In this thesis, the analysis methods derived for two-dimensional backward-wave transmission-line networks are developed for the generalized three-dimensional case, and the results are verified with numerical simulations and measurements. A way of coupling electromagnetic fields between a transmission-line network and a homogeneous medium surrounding such a network is proposed and the operation of this coupling method is verified with numerical simulations.

The idea of tailoring material properties to obtain electromagnetic cloaking of scattering objects has been extensively studied in the recent literature. This phenomenon can be achieved with various methods. In this thesis a cloaking method based on volumetric structures composed of transmission-line networks is proposed and studied. The basic principle of cloaking and the related restrictions are analytically explained and the cloaking phenomenon is verified with numerical simulations and measurements.

Coupling of electromagnetic fields between a transmission-line network and a homogeneous medium surrounding such a network enables the utilization of these artificial materials in, for example, antenna applications. In this thesis this possibility is used in implementing microwave lenses that can mitigate the unwanted reflections that are inherent to any conventional dielectric lens.

Keywords Transmission line, backward wave, electromagnetic cloaking, scattering cross section	
ISBN (printed) 978-951-22-9986-7	ISSN (printed) 1797-4364
ISBN (pdf) 978-951-22-9987-4	ISSN (pdf) 1797-8467
Language English	Number of pages 88 + appendix 86
Publisher Helsinki University of Technology, Department of Radio Science and Engineering	
Print distribution Helsinki University of Technology, Department of Radio Science and Engineering	
☒ The dissertation can be read at http://lib.tkk.fi/Diss/2009/isbn9789512299874/	

VÄITÖSKIRJAN TIIVISTELMÄ	TEKNILLINEN KORKEAKOULU PL 1000, 02015 TKK http://www.tkk.fi

Tekijä Pekka Alitalo

Väitöskirjan nimi

Mikroaaltoalueen siirtojohtoverkot taka-aaltoväliaineisiin ja sironnan vähentämiseen

Käsikirjoituksen päivämäärä 20.3.2009	Korjatun käsikirjoituksen päivämäärä 1.7.2009
Väitöstilaisuuden ajankohta 7.8.2009	
☐ Monografia	☒ Yhdistelmäväitöskirja (yhteenveto + erillisartikkelit)

Tiedekunta	Elektroniikan, tietoliikenteen ja automaation tiedekunta
Laitos	Radiotieteen ja -tekniikan laitos
Tutkimusala	Radiotekniikka
Vastaväittäjä(t)	Professori Christophe Caloz, École Polytechnique Montréal
Työn valvoja	Professori Sergei Tretyakov
Työn ohjaaja	Professori Sergei Tretyakov

Tiivistelmä

Väitöskirjassa tutkitaan siirtojohtoverkkojen käyttöä erilaisissa rakenteissa ja laitteissa jotka omaavat eksoottisen vasteen näihin kohdistuviin sähkömagneettisiin kenttiin. Tutkimuksen pääkohteet ovat väliaineet joissa esiintyy taaksepäin eteneviä aaltoja, rakenteet jotka pystyvät sähkömagneettiseen verhoamiseen, eli kappaleiden kokonaissirontapoikkipinnan pienentämiseen, sekä uusi tapa toteuttaa mikroaaltoalueen linssejä volumetristen siirtojohtoverkkojen avulla.

Väliaineissa joissa esiintyy taaksepäin eteneviä aaltoja sähkömagneettisten aaltojen vaihe etenee vastakkaiseen suuntaan energian kanssa. Tällaiset väliaineet voivat olla erittäin hyödyllisiä johtuen tietyistä eksoottisista ilmiöistä, kuten negatiivisesta taitekertoimesta ja vaimenevien aaltojen amplitudin resonoivasta kasvattamisesta, jotka mahdollistavat kuvantamisen aallonpituutta tarkemmalla resoluutiolla. Tässä väitöskirjassa kaksiulotteisille siirtojohtoverkoista koostuville taka-aaltoväliaineille johdetut analyysimenetelmät kehitetään yleisemmälle kolmiulotteiselle tapaukselle ja nämä tulokset vahvistetaan numeerisin simuloinnein ja mittauksin. Menetelmä sähkömagneettisten kenttien kytkemiseksi siirtojohtoverkon ja sitä ympäröivän homogeenisen materiaalin välillä esitetään ja tämän menetelmän toimivuus vahvistetaan numeerisin simuloinnein.

Ajatusta materiaalien ominaisuuksien muokkaamisesta paljon sirottavien kappaleiden verhoamiseksi on tutkittu laajalti viimeaikaisessa kirjallisuudessa. Tällainen verhoamisilmiö on mahdollista saavuttaa erilaisin menetelmin. Tässä väitöskirjassa esitetään ja tutkitaan menetelmää joka perustuu siirtojohtoverkkoihin. Tämän verhoamismenetelmän toimintaperiaatteet sekä tälle menetelmälle ominaiset rajoitteet selitetään analyyttisesti ja verhoamisilmiö vahvistetaan numeerisin simuloinnein sekä mittauksin.

Sähkömagneettisten kenttien kytkeminen siirtojohtoverkon ja sitä ympäröivän homogeenisen materiaalin välillä mahdollistaa näiden keinotekoisten materiaalien hyödyntämisen esimerkiksi antennisovelluksissa. Tässä väitöskirjassa tätä mahdollisuutta käytetään siirtojohtoverkoista koostuvien mikroaaltolinssien toteuttamiseen. Tällaiset linssit kykenevät vähentämään perinteisille dielektrisille linsseille tyypillisiä, linssin toiminnalle haitallisia heijastuksia.

Asiasanat Siirtojohto, taka-aalto, sähkömagneettinen verhoaminen, sirontapoikkipinta

ISBN (painettu) 978-951-22-9986-7	ISSN (painettu) 1797-4364
ISBN (pdf) 978-951-22-9987-4	ISSN (pdf) 1797-8467
Kieli Englanti	Sivumäärä 88 + liitteet 86

Julkaisija Teknillinen korkeakoulu, Radiotieteen ja -tekniikan laitos

Painetun väitöskirjan jakelu Teknillinen korkeakoulu, Radiotieteen ja -tekniikan laitos

☒ Luettavissa verkossa osoitteessa http://lib.tkk.fi/Diss/2009/isbn9789512299874/

Preface

This thesis is a result of the research work done under the supervision of Professor Sergei Tretyakov, at the Department of Radio Science and Engineering (former Radio Laboratory) of the Helsinki University of Technology (TKK). At the end of this thesis work, during the second half of the year 2008, the author worked as an invited researcher in the group of Professor Juan Mosig at the Laboratory of Electromagnetics and Acoustics of the École Polytechnique Fédérale de Lausanne (EPFL), Switzerland.

My warmest thanks and gratitude go to the supervisor of this thesis, Professor Sergei Tretyakov. The position in your highly appreciated and international research group has given me a great chance to work with the best scientists and experts in the field of this research. This thesis would not have been possible without your constant guidance, ideas, and help.

During my earlier research work that started already as an undergraduate student, I had the privilege of working with Dr. Stanislav Maslovski, who has had a huge impact on this thesis. Stanislav, thank you for all the help, discussions, and supervision of my work. I have also had the chance to work with many other great scientists both at TKK and at EPFL. My sincere gratitude and special thanks for all the joint work, discussions, and guidance go to Professor Juan Mosig, Professor Constantin Simovski, Professor Igor Nefedov, Professor Ari Sihvola, and Dr. Mikhail Lapine. I also wish to thank Mr. Olli Luukkonen, Dr. Frédéric Bongard, Dr. Liisi Schulman, Dr. Sylvain Ranvier, Mr. Joni Vehmas, Mr. Jukka Venermo, and Mr. Jean-Francois Zürcher for joint work in the articles that are included in this thesis. Mr. Eino Kahra and Mr. Lauri Laakso deserve special thanks for helping me in manufacturing issues.

I wish to thank Professor Andrea Alù and Professor Min Qiu for reviewing this thesis and for their valuable comments and suggestions.

During this thesis work I have received financial support from the Finnish Graduate School in Electronics, Telecommunications, and Automation (GETA), the Nokia Foundation, the Emil Aaltonen's Foundation, Tekniikan Edistämissäätiö, Elektroniikkainsinöörien Säätiö, and the European Cooperation in the Field of Scientific and Technical Research (COST). All this support is most gratefully acknowledged.

Mom and dad, thank you for your support and encouragement during the whole course of my studies.

Thank you, Martta, for all your love and constant support. Helmi and Saimi, thank you for bringing so much joy and happiness into my life.

Otaniemi, July 1, 2009, Pekka Alitalo

Contents

List of Publications

This thesis consists of an overview and of the following publications which are referred to in the text by their Roman numerals.

I P. Alitalo, S. Maslovski, and S. Tretyakov, "Three-dimensional isotropic perfect lens based on LC-loaded transmission lines," *Journal of Applied Physics*, vol. 99, no. 6, p. 064912, 2006.

II P. Alitalo, S. Maslovski, and S. Tretyakov, "Experimental verification of the key properties of a three-dimensional isotropic transmission-line superlens," *Journal of Applied Physics*, vol. 99, no. 12, p. 124910, 2006.

III P. Alitalo and S. Tretyakov, "Subwavelength resolution with three-dimensional isotropic transmission-line lenses," *Metamaterials*, vol. 1, no. 2, pp. 81–88, 2007.

IV P. Alitalo, O. Luukkonen, and S. Tretyakov, "A three-dimensional backward-wave network matched with free space," *Physics Letters A*, vol. 372, no. 15, pp. 2720–2723, 2008.

V P. Alitalo, F. Bongard, J. Mosig, and S. Tretyakov, "Backward-wave slab with electrically tunable index of refraction," *Proceedings of the 3rd European Conference on Antennas and Propagation (EuCAP 2009)*, Berlin, Germany, March 23–27, 2009, pp. 1667–1671.

VI P. Alitalo, O. Luukkonen, L. Jylhä, J. Venermo, and S. A. Tretyakov, "Transmission-line networks cloaking objects from electromagnetic fields," *IEEE Transactions on Antennas and Propagation*, vol. 56, no. 2, pp. 416–424, 2008.

VII P. Alitalo, S. Ranvier, J. Vehmas, and S. Tretyakov, "A microwave transmission-line network guiding electromagnetic fields through a dense array of metallic objects," *Metamaterials*, vol. 2, no. 4, pp. 206–212, 2008.

VIII P. Alitalo, F. Bongard, J.-F. Zürcher, J. Mosig, and S. Tretyakov, "Experimental verification of broadband cloaking using a volumetric cloak composed of periodically stacked cylindrical transmission-line networks," *Applied Physics Letters*, vol. 94, no. 1, p. 014103, 2009.

IX P. Alitalo, O. Luukkonen, F. Bongard, J.-F. Zürcher, J. R. Mosig, and S. A. Tretyakov, "Broadband cloaking of selected objects in the microwave regime with a volumetric cloak comprising layered networks of transmission lines," *Proceedings of the IEEE International Symposium on Antennas and Propagation*, Charleston, USA, June 1–5, 2009, p. 222.2.

X P. Alitalo, O. Luukkonen, J. R. Mosig, and S. A. Tretyakov, "Broadband cloaking with volumetric structures composed of two-dimensional transmission-line networks," *Microwave and Optical Technology Letters*, vol. 51, no. 7, pp. 1627–1631, 2009.

XI P. Alitalo, O. Luukkonen, J. Vehmas, and S. A. Tretyakov, "Impedance-matched microwave lens," *IEEE Antennas and Wireless Propagation Letters*, vol. 7, pp. 187–191, 2008.

XII P. Alitalo, F. Bongard, J. Mosig, and S. Tretyakov, "Transmission-line lens antenna with embedded source," *Proceedings of the 3rd European Conference on Antennas and Propagation (EuCAP 2009)*, Berlin, Germany, March 23–27, 2009, pp. 625–629.

Author's contribution

In all the papers [**I**–**XII**] the author of this thesis had the main responsibility in developing and writing the papers. More detailed contributions are indicated below.

Paper [**I**] resulted from the author's Master's thesis. The derivations, calculations, design, and simulations were carried out by the author under the supervision of Dr. Stanislav Maslovski and Professor Sergei Tretyakov. Dr. Stanislav Maslovski gave valuable guidance in the derivation of the analytical formulas. The idea of the realization of three-dimensional transmission-line networks with coaxial transmission lines as proposed in [**I**] was Dr. Stanislav Maslovski's.

Paper [**II**] resulted from the author's Master's thesis. The author carried out the calculations, design, manufacturing, and measurements under the supervision of Dr. Stanislav Maslovski and Professor Sergei Tretyakov.

The author formulated the idea and carried out the derivations, calculations, design, and simulations in [**III**] under the supervision of Professor Sergei Tretyakov.

The author formulated the idea and carried out the derivations, calculations, and structure design in [**IV**]. The numerical simulations were done by the author together with Mr. Olli Luukkonen. The method of coupling the studied transmission-line network with a homogeneous medium was developed by the author. Professor Sergei Tretyakov supervised the work.

The author formulated the idea and carried out the design and simulations in [**V**]. Dr. Frédéric Bongard conducted the evaluation of the effective values of the lumped elements used in the simulation model. The work was supervised by Professor Juan Mosig and Professor Sergei Tretyakov.

The derivations, structure design, and part of the simulations in [**VI**] were carried out by the author under the supervision of Professor Sergei Tretyakov, who also formulated the original idea of the paper. The numerical simulations of the transmission-line structure were carried out by the author together with Mr. Olli Luukkonen. Dr. Liisi Schulman (née Jylhä) conducted the FDTD simulations and Mr. Jukka Venermo the scattering simulations that were done with the COMSOL Multiphysics software. The method of coupling the studied transmission-line network with a homogeneous medium was developed by the author.

The author formulated the idea, designed the measurement setup, and carried out the measurements and the numerical simulations in [**VII**], under the supervision of Professor Sergei Tretyakov. Dr. Sylvain Ranvier programmed the software controlling the scanners used in the measurements and Mr. Joni Vehmas helped in manufacturing and testing of the measurement setup.

The author formulated the idea and carried out the design and simulations in [**VIII**]. Manufacturing and assembly of the experimental setup were done by the author together with Mr. Jean-Francois Zürcher and Dr. Frédéric Bongard. The measurements were conducted by the author together with Dr. Frédéric Bongard. The work was supervised by Professor Juan Mosig and Professor Sergei Tretyakov.

The author formulated the idea and carried out the design and simulations in [**IX**]. Mr. Olli Luukkonen helped in writing of the paper. Manufacturing and assembly of the experimental setup were done by the author together with Mr. Jean-Francois Zürcher and Dr. Frédéric Bongard. The measurements were conducted by the author together with Dr. Frédéric Bongard. The work was supervised by Professor Juan Mosig and Professor Sergei Tretyakov.

The author formulated the idea and carried out the structure design in [**X**]. The numerical simulations were done by the author together with Mr. Olli Luukkonen. The work was supervised by Professor Juan Mosig and Professor Sergei Tretyakov.

The derivations, calculations, and simulations in [**XI**] were carried out by the author. Mr. Olli Luukkonen and Mr. Joni Vehmas helped with the numerical simulations. Professor Sergei Tretyakov formulated the original idea of the paper and supervised the work.

The author formulated the idea and carried out the design in [**XII**]. The numerical simulations were done by the author together with Dr. Frédéric Bongard. The work was supervised by Professor Juan Mosig and Professor Sergei Tretyakov.

In addition to the papers listed above, the author of this thesis has contributed in several other journal and conference papers in the field of this research, including an invited review paper on the topic of electromagnetic cloaking. References to these publications are included in the thesis.

List of Abbreviations

BW	Backward wave
DNG	Double negative (medium)
FW	Forward wave
LH	Left handed (medium)
NRI	Negative refractive index (medium)
PMC	Perfect magnetic conductor
SCS	Scattering cross section
TL	Transmission line
TLM	Transmission-line matrix

List of Symbols

A, B, C, D	Components of a transmission matrix
C	Capacitance
d	Unit cell size of a periodic structure
$\overline{E}$	Electric field (vector)
F	Focal distance
f	Frequency
$\overline{H}$	Magnetic field (vector)
I	Current
j	Imaginary unit
$\overline{k}$	Wave vector
k	Wavenumber
k_0	Wavenumber in free space
k_{eff}	Effective wavenumber
k_t	Transverse wavenumber
$k_{t,\max}$	Maximum transverse wavenumber contributing to an image
k_{TL}	Wavenumber of waves travelling in a transmission line
k_x, k_y, k_z	Components of the wave vector
L	Inductance
l	Thickness of a backward-wave slab
n	Refractive index, integer
P_{INC}	Incident power
$P_{\text{SCA,BW}}$	Power scattered in the backward direction
$P_{\text{SCA,FW}}$	Power scattered in the forward direction
R_{e}	Resolution enhancement
S_{11}	Reflection coefficient
S_{21}	Transmission coefficient
T	Lens thickness
V	Voltage
x, y, z	Position coordinates
Y	Admittance
Y_{load}	Load admittance
Z	Impedance, characteristic impedance
Z_B	Bloch impedance
Z_{load}	Load impedance
Z_{TL}	Characteristic impedance of a transmission line

γ	Propagation constant
Δ	Image resolution
ε	Permittivity
ε_0	Permittivity of free space
ε_r	Relative permittivity
$\varepsilon_{\mathrm{eff,TL}}$	Effective relative permittivity of a transmission line
η	Wave impedance
η_0	Wave impedance of free space
θ	Electrical length of a transmission line, angle
λ	Wavelength
λ_eff	Effective wavelength
μ	Permeability
μ_0	Permeability of free space
μ_r	Relative permeability
ρ	Reflection coefficient
τ	Transmission coefficient
ϕ	Angle
ω	Angular frequency

List of Figures

1 Introduction

The electromagnetic response of a material is defined by the properties, such as permittivity and permeability, of this material. The design of devices that utilize electromagnetic field phenomena is based on knowing how the material in question behaves when electromagnetic fields are applied to it. Different natural and man-made electromagnetic materials are used for various purposes, such as insulators and conductors in electronic devices. The recent development of so-called metamaterials has opened new possibilities to design materials taylored for specific purposes. By definition, metamaterials differ from other man-made materials by having electromagnetic properties that are not readily found in nature. Because of the fact that an engineer is not anymore restricted by the values of the materials' electromagnetic constitutive parameters that are readily available in nature, he or she is free to design conventional devices in a new, and possibly more advantageous way. Furthermore, many aspects of metamaterials may result in not only improvement of conventional devices, but in the creation of whole new classes of devices for various applications.

In this thesis, the design and use of so-called transmission-line networks is considered as an option to create structures that enable exotic and unnatural, or otherwise beneficial type of wave propagation, and most importantly, allow free design of the electromagnetic response of the structure. The thesis consists of three specific research directions. First, the design and development of three-dimensional transmission-line networks for structures supporting backward waves are considered. This work is a generalization of the well-known concepts of one- and two-dimensional periodically loaded transmission-line networks. Furthermore, a novel way of coupling these types of networks to the surrounding medium, such as free space for example, is presented. The introduction of these coupling structures is very important in enabling the use of transmission-line networks in applications that require free propagation of electromagnetic waves in the medium surrounding the transmission-line networks, such as many antenna applications do. Within this thesis, three-dimensional loaded transmission-line networks, exhibiting backward-wave propagation characteristics, are studied analytically and numerically, and the main results are confirmed with experiments.

Second, the development and design of structures capable of electromagnetic cloaking, i.e., reducing the scattering and absorption of impinging electromagnetic waves, are considered. This topic in general has aroused rapidly increasing interest in the scientific community during the past few years. The goal of this research direction is to study structures that can be used for decreasing the total scattering cross section of various objects. In the ideal case, an object can be placed inside the cloak structure in such a way that all scattering is removed. This basically means that the object and the cloak structure are made invisible to the surrounding electromagnetic fields. Within this thesis work, cloaking based on volumetric networks of

transmission lines is proposed and studied analytically, numerically, and experimentally. This approach has many benefits as compared to other cloaking techniques, for example the simplicity of design and manufacturing, and wide operation bandwidth.

The third research direction is the introduction of a novel approach to the realization of microwave lenses, enabling the creation of low-loss microwave lenses to be used, for example, in antenna applications. Also here the use of volumetric transmission-line networks plays a key role, as the proposed lenses are effectively artificial materials composed of such networks.

The research methods used in this thesis include analytical, numerical, and experimental work. Analytical equations are derived for the study of wave propagation and impedance in various structures. Numerical simulations are conducted for the verification of the predicted theoretical models and for the study and optimization of different types of structures. Operation of some of the designed structures and devices are confirmed with measurements.

The rest of the thesis is organized in the following manner:

Chapter 2 gives a general overview of the subject of metamaterials and of three specific topics related to such materials, namely, backward-wave media, electromagnetic cloaking, and antenna applications.

Chapter 3 reviews the background of the analysis of periodic structures and transmission-line networks. The methods discussed in this chapter form the basis of the theoretical analysis presented in this thesis.

Chapter 4 and papers [**I**–**V**] present and discuss the results of the thesis that are related to the study of three-dimensional transmission-line networks exhibiting backward-wave propagation characteristics. The existing literature related to this topic is also reviewed.

Chapter 5 and papers [**VI**–**X**] present and discuss the results of the thesis on the topic of electromagnetic cloaking. Alternative approaches to electromagnetic cloaking are also discussed.

Chapter 6 and papers [**XI**,**XII**] present and discuss the results of the thesis that are related to microwave lens design. A novel way of creating lenses with mitigated reflections is presented and studied. Alternative ways of reducing reflections in microwave lenses are discussed.

Conclusions of the thesis are given in Chapter 7.

2 Metamaterials

2.1 General

The definition of the term "metamaterial" varies in the literature, but most often it is used to describe an artificial material that has exotic electromagnetic properties [1–6]. Usually these properties are defined by the constitutive parameters of a material, such as permittivity ε and permeability μ. For detailed discussions on the terminology of metamaterials, see, e.g., [4] and the references therein. In this thesis we choose to use the definition adopted in [3]: a metamaterial is "an artificial effectively homogeneous electromagnetic structure with unusual properties not readily available in nature."

To look more closely what this definition really means, let us explain the meaning of the words in this definition more precisely. "Artificial effectively homogeneous" simply means that the material is artificial (man-made) but that it behaves effectively as a homogeneous material. To satisfy the latter condition, the cell size of the microstructure of the material must be considerably smaller than the wavelength of electromagnetic radiation inside the material. Since the wavelength depends inversely on the frequency of the radiation, we can conclude that a metamaterial may not be a homogeneous material at some frequencies. There is no strict rule on the limit of the cell size where a structure becomes effectively homogeneous. In [3] the following rule of thumb is given: if the guided wavelength, i.e., the wavelength of electromagnetic radiation in the material, is larger than 4 times the microstructure cell size, the material can be treated as being effectively homogeneous. The literature and various approaches to the homogenization of artificial materials is extensive, see, e.g., [7] and the references therein.

Looking at the second part of the previous definition of a metamaterial, we can conclude that for a material to be metamaterial, it cannot be *readily* found in nature. This definition is very appropriate since it is not too strict in demanding that a phenomenon related to a specific metamaterial is not found in nature at all. Many natural electromagnetic phenomena, such as occurs for example in plasma, can be thought of being very exotic. They are simply not occurring in environments or in materials that can be used in a specific application within a convenient frequency range.

Artificial electromagnetic materials have been known since the 1940's, when it was found that by combining metallic particles in a host dielectric, an artificial material could be created [8, 9]. Of course, this "material" can be identified only at frequencies where the wavelength is large enough as compared to the structural period of the material. This type of material, however, is not a metamaterial according to our previous definition, since dielectrics with such properties as those used in [8, 9] can be readily found in nature. Usually the motivation in creating these types of

artificial dielectrics is that even though they do not possess any exotic electromagnetic properties, they have some advantage over the natural materials having similar electromagnetic properties. This advantage can be for example reduction of weight.

In radio engineering the metamaterials may find many applications since the used frequencies are relatively low and the wavelength relatively large, thus enabling the production of composite materials with enough accuracy. As an example, the microwave region is usually defined to be up to the frequency 300 GHz, where the wavelength in free space is 1 mm. This wavelength can be still considered large enough for the manufacturing of artificial materials having inclusions with a period much less than the wavelength. It must be noted though that the free space wavelength should not always be used as a measure when looking at the possibility to homogenize a material since the wavelength inside the material is the defining factor. Thus, there is no strict rule on the frequency limits of realizable metamaterials, since the material properties define the wavelength. Also, various manufacturing technologies are continuously developed which are pushing the obtainable frequencies higher all the time.

The research related to metamaterials has been constantly increasing in the 21st century and has resulted in a large number of scientific publications. The various research directions, applications, and main results have been discussed and reviewed in several monographs [1–3, 10–17]. From these, the most relevant books regarding the specific topics discussed in this thesis are [1–3], since [1] includes a general review on the principles of modelling of composite materials, and the books [2, 3] concentrate on the concept of transmission-line metamaterials.

2.2 Backward-wave media

Perhaps the most studied special cases of metamaterials are the backward-wave (BW) media having negative permittivity ε and permeability μ. They are often also called negative-refractive-index (NRI) media, double-negative (DNG) media or left-handed (LH) media [2, 3]. This type of medium was first theoretically studied by Veselago in 1967 [18]. In the 21st century the subjects of metamaterials and especially backward-wave materials have aroused continuously increasing amount of interest after the publications containing the idea of a composite material with simultaneously negative permittivity and permeability by Smith *et al.* [19], the first experimental demonstration of negative refraction by Shelby *et al.* [20], and a theoretical study on the possibility of super-resolution by Pendry [21].

In a backward-wave medium the wave vector is antiparallel to the Poynting vector [1, 18,22]. Basically, this means that the phase propagates in the opposite direction with respect to the energy. This effect, not found in any natural homogeneous material, has some interesting consequences on the behavior of electromagnetic fields in these type of media. For instance, when an electromagnetic wave penetrates an interface

between a backward-wave medium and a medium with positive ε and μ (FW or forward-wave medium, such as free space), the wave refracts negatively [23, 24] as can be concluded by applying the Snell's law to such an interface.

The first experimental demonstration of a backward-wave medium was realized with a metamaterial composed of metallic wires and metallic ring-shaped resonators called split-ring resonators [19, 20]. In this case, the effectively negative ε is due to the metallic wires, having a Drude-type dispersion (e.g. [25]) that allows for negative values of ε. The effectively negative μ, having a Lorentz-type dispersion (e.g. [25]), is realized by designing the resonators in such a way that at a certain frequency, the resonators exhibit a strong magnetic resonance, allowing the effective μ to have negative values. The concept of artificial magnetic materials made from metal inclusions with various shapes (broken loops in many cases) have been widely studied in the literature [26–29].

Due to the inherently dispersive and resonant material parameters, the backward-wave metamaterials realized with broken loops have, in most cases, very high losses and narrow bandwidth. Despite of this, the negative refraction of an electromagnetic beam through a prism-type metamaterial block was experimentally demonstrated [20]. After this, also others have given further experimental verification of this phenomenon, e.g., [30, 31]. Metamaterials, and especially backward-wave materials based on the use of resonant inclusions such as those in [20], have been widely studied and further developed in the recent literature, see, e.g., [4] and the references therein.

One very special property of backward-wave materials is that a parallel-sided slab of such a material, when the material properties are designed to meet certain specifications, can act as a so-called "superlens" [1, 21]. An idealized superlens, which is sometimes called "perfect lens", is a device that can focus a point-source field to an infinitely small area. This means an imaging device that has infinitely high resolution, i.e., infinitely small details of the source field can be recognized in the image plane of the device. It is well known that the classical limit of image resolution is in the order of the wavelength of the used electromagnetic radiation [32]. This is due to the fact that the evanescent waves, that carry the information of the sub-wavelength details of the source, are in any media exponentially decaying as a function of the distance. This means that in any image which is not in the very near-field of the source, only propagating modes add information, and this results in that the image resolution is approximately

$$\Delta \approx 2\pi \frac{1}{k_{t,\max}} \approx 2\pi \frac{1}{k} = 2\pi \frac{\lambda}{2\pi} = \lambda, \tag{2.1}$$

where $k_{t,\max}$ is the maximum transverse wavenumber contributing to the image, k is the wavenumber in the medium where the wave travels, and λ is the wavelength. A superlens is capable of "amplifying" the decaying evanescent modes and, in the ideal case, preserving the information carried by these modes in the image [1, 21].

According to the above discussion it is clear that a superlens differs greatly from any conventional lens. Traditionally, the word "lens" is used for a device that can focus for example a plane wave into a focal spot. A superlens cannot achieve this, the waves that are normally incident to the superlens slab are simply transmitted through the slab without any refraction. Instead, a superlens can achieve imaging of, e.g., a point source as depicted in Fig. 2.1.

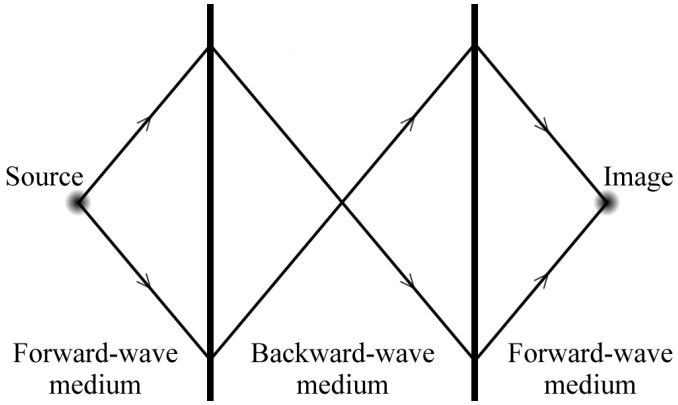

Figure 2.1: Imaging of propagating waves in a parallel-sided slab of a backward-wave medium, sandwiched between two regions of forward-wave medium. The thin lines illustrate how two rays are refracted negatively at the slab interfaces and form an image on the other side of the slab. Another image is formed inside the slab. The arrows indicate the power propagation direction.

But negative refraction refers only to the propagating modes impinging on an interface and as such does not result in any sub-wavelength resolution in the image. Instead, the high resolution obtainable with a slab made of a backward-wave medium relates to the resonant "amplification" of the evanescent modes which can occur at the interfaces between the slab and the (forward-wave) medium surrounding the slab. This is made possible by the fact that such interfaces can support surface waves with large wavenumbers and these can be resonantly enhanced, therefore "amplifying" the evanescent fields [1]. It must be noted that causality and energy conservation laws are not violated by such enhancement of fields, since the evanescent modes do not carry energy.

If a backward-wave slab is sandwiched between regions of a forward-wave medium and if the permittivity and permeability of the slab are exactly the negative of those in the forward-wave medium, the evanescent modes excited by a source (placed in the forward-wave medium) are enhanced at the interfaces of the slab in such a way that the amplitudes of all these exponentially decaying modes are exactly the same in the image plane and in the source plane, as shown in Fig. 2.2. This idealized situation is hardly the case in any realistic structure, where losses can easily suppress the enhancement of the evanescent modes. Nevertheless, the possibility of obtaining

imaging with sub-wavelength resolution, even though not ideal resolution, would be a major improvement in many practical technological issues related to imaging, production of miniaturized devices and components, data storage, etc.

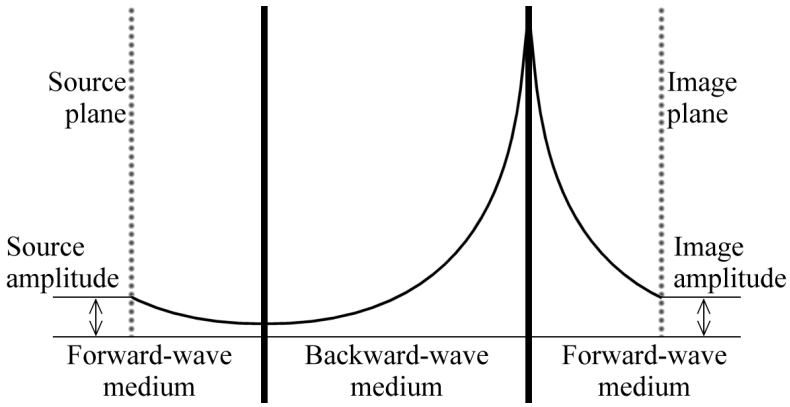

Figure 2.2: Behavior of the amplitude of the evanescent fields in a backward-wave slab and the surrounding forward-wave medium. Resonant amplification of the evanescent modes results in the restoration of the source field's amplitude at the image plane.

Regardless of the lack of an optical axis, which is traditionally been related to any type of lens, the name "superlens" has achieved a wide acceptance in the literature and in the electromagnetics community, so in this thesis we also use the name "superlens" to describe a parallel-sided slab composed of a backward-wave medium.

One research area of this thesis is the study of three-dimensional structures exhibiting backward-wave propagation properties in a certain frequency range. Chapter 4 presents a design technique and a class of such structures developed within this thesis. These structures are composed of three-dimensionally arranged transmission-line networks that are periodically loaded by reactive loads enabling backward-wave propagation in the networks. Also other results regarding three-dimensional backward-wave transmission-line networks have been presented in the recent literature. These alternative techniques are also reviewed in Chapter 4.

2.3 Electromagnetic cloaking

Recently, the topics of electromagnetic cloaking and invisibility have become major subjects of metamaterial-related research after the publication of some seminal works by Alù, Engheta, Leonhardt, and Pendry *et al.* [33–35]. The term "electromagnetic cloaking" refers to the reduction of the total scattering cross section of an object, meaning in the ideal case that this object is made invisible to the impinging

electromagnetic radiation. This strongly differs from previously well known methods for scattering reduction, for example the stealth technology, since in cloaking the goal is to minimize the total scattering, not just scattering to certain directions.

Reduction of forward scattering essentially means that an electromagnetic wave can "see" behind the cloaked object, as the object is "invisible" to the wave impinging on this object. See Fig. 2.3 for an illustration of the main idea of cloaking, where a system of two antennas is considered. The scattering from an object placed between these antennas is depicted in three different cases: scatterer alone, scatterer surrounded by an ideally absorbing material, and scatterer inside an ideal cloak. In the first case (Fig. 2.3a) the object scatters both towards the source (backscattering) and towards the receiving antenna (forward scattering). In the second case (Fig. 2.3b) all the power incident to the object is absorbed. This removes the power reflected back to the source but the forward scattering remains since behind the object a shadow is created. In the last case (Fig. 2.3c), where all the scattering is removed, the signal at the receiving antenna is the same as would be without any object between the antennas.

To obtain cloaking of an object, the total power that is scattered by this object should be somehow minimized, as illustrated in Fig. 2.3. The use of an absorbing material can reduce the total scattering cross section, but only by a maximum amount of 50 %, since the forward scattering cannot be reduced by absorbing [36]. The only way to reduce both backscattering and forward scattering is to somehow change the field pattern around the object to be cloaked. This should be done in a way that the fields around the scattering object (in both near- and far-fields) would resemble the fields that would exist there without this object.

Cloaking can be achieved in many ways. Although being a very popular subject of research only since a few years, there exist publications strongly related to this field of research dating back even several decades [37–40]. During the past few years, this area of research has become extremely popular as several new concepts and ideas have been presented [33–35].

Chapter 5 discusses a cloaking technique which has been developed within this thesis work. This route to electromagnetic cloaking takes advantage of a property inherent to many types of transmission lines: the fields propagating inside a transmission line are confined there, thus enabling the "squeezing" of fields into a set of transmission lines (or more precisely, into a network composed of transmission lines). In Chapter 5 principles of this cloaking approach, together with design and realization examples are presented. Also two of the recently most widely referenced cloaking techniques, namely, the scattering cancellation technique and the coordinate-transformation technique are reviewed in Chapter 5. Other cloaking techniques are briefly explained and references to these are also given.

Even though being a relatively new area of research, the subject of electromagnetic cloaking has already resulted in a huge amount of publications. Recent review

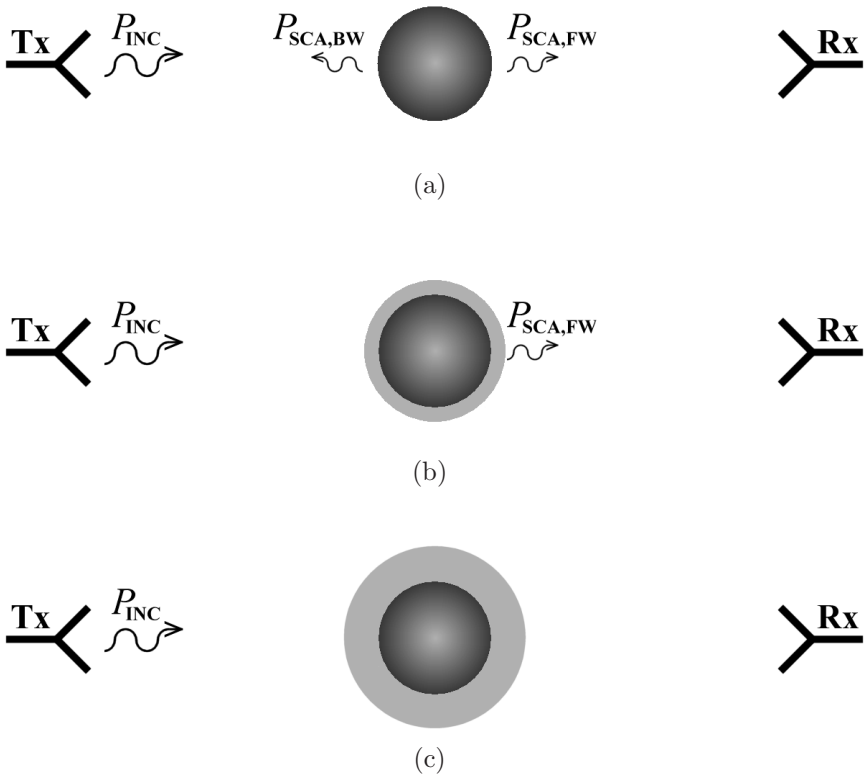

Figure 2.3: A system of two antennas: a transmitting antenna (Tx) and a receiving antenna (Rx). (a) A scattering object is placed between the antennas. (b) A scattering object covered with a perfectly absorbing material is placed between the antennas [only backscattering is removed as compared to case (a)]. (c) A scattering object placed inside a hypothetical, idealized cloak is placed between the antennas [all scattering is removed as compared to case (a)].

papers on this topic summarize the current research directions, latest developments and future prospects [41,42]. Review paper [42] has been written by the author and supervisor of this thesis and that paper is in a large part a result of the work done for this thesis during the last few years.

2.4 Artificial materials in antenna applications

An important application area of artificial dielectrics and metamaterials is antennas. The potential benefits in this field of engineering, offered by various artificial materials include, for example, improvement of directivity and bandwidth characteristics of conventional antennas and antenna miniaturization [2,3,10]. Completely

new types of antennas have also been introduced. Good examples of these are leaky-wave antennas based on backward-wave propagation [2, 3].

Artificial dielectrics and their use in lenses have been known since the 1940's, see, e.g., [8, 9, 43]. The introduction of various ways of creating metamaterials exhibiting both electric and magnetic response (materials with the relative permittivity $\varepsilon_{\mathrm{r}} \neq 1$ and relative permeability $\mu_{\mathrm{r}} \neq 1$) has opened up the possibility to dramatically improve antenna substrates, superstrates, and lenses since in such magneto-dielectric materials both the refractive index and the impedance can be engineered [44–46]. The problems in the realization and application of magneto-dielectric materials are related to difficulties in obtaining magnetic response from low-loss artificial materials in a wide frequency band. Indeed, most of the magneto-dielectric materials that have been studied in the literature, have suffered from strong dispersion and high losses, especially in the frequency ranges where the magnetic response is required [47, 48].

Chapter 6 presents how transmission-line networks can be used as microwave lenses. Although magnetism, neither natural or artificial, is not involved, the impedance matching characteristics, as compared to conventional dielectric lenses, are shown to be improved. The lens structures studied in Chapter 6 cannot be considered to be metamaterials in the strict definition of the term, since these lenses are merely artificial materials for which the coupling between the lens material and the surrounding homogeneous medium is improved by the use of a special coupling layer. Other ways of reducing reflections from dielectric lenses are also briefly explained in Chapter 6.

3 Transmission-line networks

3.1 General

Transmission-line networks are periodic structures composed of transmission lines. These types of structures are well known in radio engineering since many homogeneous materials and periodic structures can be conveniently analyzed using equivalent transmission-line models that are simple to use and in most cases model accurately the wave propagation phenomena in such materials and structures. The theory of periodic structures and their analysis using equivalent transmission-line models are therefore well established, see, e.g. [49, 50].

The use of structures composed of periodic networks of transmission lines has recently become popular since many exotic electromagnetic phenomena, such as negative refraction, achievable only with metamaterials, can be found in these periodic transmission-line "materials" [2, 3]. The most significant benefits of using transmission-line based structures instead of, e.g., composite materials made of separate inclusions, are the wide bandwidths, the ease of manufacturing, and the tolerance to losses. The latter is especially significant when it comes to backward-wave materials, which are very lossy when they contain separate resonant inclusions such as split-ring resonators [19].

Caution should be used when describing transmission-line networks as "materials." Although a network of transmission lines can be considered to have propagation properties similar as a homogeneous material with certain effective material constituents ε and μ, the network may have severe limitations for polarization and the way the fields can be excited inside the network. The latter limitation is significant only in cases where the transmission-line "material" needs to be coupled with another material surrounding the network, free space for example. This is the case in any application that requires that the source is outside the network.

Metamaterials have been suggested to offer many benefits for example in imaging and antenna applications. Many examples of such artificial materials, in both planar and three-dimensional form, have been proposed for these applications, acting as antenna superstrates, substrates, or lenses. These applications are good examples of cases where the sources of electromagnetic fields are usually situated outside the metamaterial. Therefore, the metamaterial needs to be designed in such a way that the fields emitted by a source are coupled into the material in a desired way. But in many cases this requirement is not very demanding, e.g., when an antenna acting as a source emits radiation of only one polarization.

When the transmission-line approach to metamaterial design was first introduced, the "materials" were usually composed of one-dimensional or two-dimensional periodic networks of transmission lines, realized for example with the microstrip technol-

ogy [51–58]. These types of networks obviously cannot be considered as materials in the traditional sense, since an impinging electromagnetic wave hardly couples with such networks. Instead, the proposed applications of these types of networks included devices that permitted direct excitation of the networks. Such devices include, e.g., phase shifters, power dividers, and various types of antennas [2, 3].

3.2 Analysis methods

Principles of analysis of periodic structures have been presented, e.g., in [49,50]. The analysis relies on the Floquet theorem which is a basic theorem for wave propagation in a periodic structure. The theorem states that if a function $\overline{E}(x, y, z)$ satisfies the wave equation of a wave propagating along the z-direction in a periodic structure, then the function $\overline{E}(x, y, z + nd)$, where d is the period of the structure and n any integer number, can be represented as

$$\overline{E}(x, y, z + nd) = \overline{E}(x, y, z)e^{-\gamma nd}, \tag{3.1}$$

where the propagation constant γ is a complex coefficient. In practice (3.1) means that in the periodic structure the field between any positions z and $z + nd$ varies only by a complex multiplier.

Another useful way of describing wave propagation in periodic transmission-line structures is to use the so-called ABCD-parameters [49,50]. These parameters relate the currents I and voltages V at both sides of the unit cell to each other as

$$\begin{bmatrix} V_n \\ I_n \end{bmatrix} = \begin{bmatrix} A & B \\ C & D \end{bmatrix} \begin{bmatrix} V_{n+1} \\ I_{n+1} \end{bmatrix} = \begin{bmatrix} V_{n+1}e^{\gamma d} \\ I_{n+1}e^{\gamma d} \end{bmatrix}, \tag{3.2}$$

where we have used relations $V_{n+1} = V_n e^{-\gamma d}$ and $I_{n+1} = I_n e^{-\gamma d}$ which follow from (3.1).

The propagation constant γ and the characteristic impedance (Bloch impedance) of a periodic structure can be conveniently analyzed by solving the ABCD-parameters. From (3.2) we can find an equation for the propagation constant γ (dispersion equation) [49]:

$$AD + e^{2\gamma d} - (A + D)e^{\gamma d} - BC = 0. \tag{3.3}$$

Also the characteristic impedance, or Bloch impedance, defined by [49]:

$$Z_B = \frac{V_{n+1}}{I_{n+1}}, \tag{3.4}$$

can be solved in terms of the ABCD-parameters (3.2).

See Fig. 3.1a for an illustration of an equivalent circuit of a periodic structure. Basically any one-dimensional periodic structure can be represented by this model, with Z_{11} being the ratio between the voltage and current at the left-side terminal and Z_{22} being the ratio of the voltage and current at the right-side terminal.

Although the circuit model in Fig. 3.1a can be used to describe any periodic one-dimensional structure, for the analysis of periodic transmission-line structures it is usually more convenient to separate the host transmission line from possible discontinuities that are placed periodically to the host transmission line. One possible representation of this type of periodic networks is shown in Fig. 3.1b. Here the host transmission line is described by its electrical length θ per period and by the series impedance Z and shunt admittance Y that correspond to the discontinuities inserted into the host transmission line. Wave propagation inside this periodic structure, assuming that the structure is infinite in the propagation direction, can be analyzed with the previously described Floquet theorem.

As already mentioned, another important design aspect of any periodic transmission-line structure is the characteristic impedance, or Bloch impedance, of this structure.

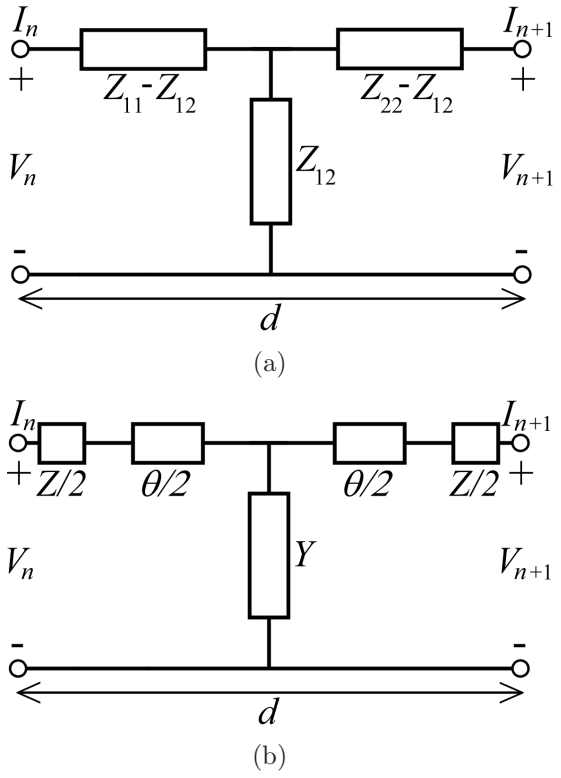

Figure 3.1: (a) Equivalent circuit of a unit cell of a periodic one-dimensional structure. (b) Equivalent circuit of a unit cell of a periodically loaded transmission-line.

If we impose a restriction that the characteristic impedance of a periodic structure is sampled only at specific points, e.g., at the terminals of the circuits in Fig. 3.1, this impedance is unique. Otherwise the impedance value changes for different sampling points inside one unit cell.

Analytical and numerical modeling methods, as well as realizations of various types of one-dimensional and two-dimensional transmission-line networks have been well established [2, 3, 51–67]. The extension of these techniques to three-dimensional structures and some novel applications of two-dimensional and three-dimensional transmission-line networks will be discussed in the following chapters.

3.3 Equivalent constitutive parameters of transmission-line metamaterials

Since homogeneous materials and periodic structures can be analyzed and emulated by equivalent transmission-line models and structures, it may be sometimes useful to describe the propagation of waves, reflection, transmission, etc. with the help of traditional constitutive parameters of materials, such as the permittivity ε and permeability μ. Let us consider a periodic one-dimensional transmission-line network with one unit cell comprising a series inductance L, a series capacitance C', a shunt inductance L', and a shunt capacitance C. The series connection of L and C' compose the series impedance Z and the parallel connection of L' and C compose the shunt admittance Y. Assuming that the period of the structure d is much smaller than the wavelength, i.e., assuming the quasi-static field condition, and applying the Maxwell's equations to find out the constitutive parameters, the following equations can be found to describe ε and μ [2, 3]:

$$\varepsilon(\omega) = \frac{Y(\omega)/d}{j\omega} = C/d - \frac{1}{\omega^2 L' d}, \tag{3.5}$$

$$\mu(\omega) = \frac{Z(\omega)/d}{j\omega} = L/d - \frac{1}{\omega^2 C' d}, \tag{3.6}$$

where ω is the angular frequency. However, such ε and μ do not necessarily model the local electric and magnetic polarizations in the structure.

From the above equations it is evident that the constitutive material parameters can be easily made either positive or negative simply by choosing the values of the reactive elements and the frequency appropriately. In a normal (forward-wave) transmission line the series inductance L and the shunt capacitance C are dominant, thus the line exhibits forward-wave propagation characteristics. If the same line is periodically loaded by series capacitance C' and shunt inductance L', effective ε and μ of the line can become negative.

3.4 Applications of transmission-line metamaterials

Transmission-line based structures and especially periodically loaded transmission-line networks exhibiting backward-wave propagation characteristics have had important influence on the metamaterial research in general. Due to the inherently low losses and the ease of manufacturing, this approach to metamaterial design has produced some important experimental verifications of many key concepts related to metamaterials. For example, the first experimental demonstration of subwavelength resolution was achieved with a planar two-dimensional capacitively and inductively loaded transmission-line network [58]. Furthermore, the easy implementation of this technique to microwave circuit design and planar antennas has resulted in a number of practical devices exploiting the special characteristics of these transmission-line based "metamaterials" [3, 68–73].

Improvements and completely new approaches enabled by the transmission-line metamaterials have been found, for example, in the design and realization of power dividers [74, 75], couplers [76, 77], phase shifters and delay lines [78–81], antenna miniaturization [82–84], and leaky-wave antennas [85–88].

4 Three-dimensional forward- and backward-wave transmission-line networks

4.1 Introduction

Recently published works on one- and two-dimensional transmission-line networks have given an interesting alternative for metamaterial design [2, 3, 51–56]. Most importantly, the ease of manufacturing due to the possibility of using planar technologies and the absence of the need to use resonant inclusions in backward-wave media have opened up a possibility to use metamaterials in many applications requiring cheap components and broadband response. In order to increase the scope of these transmission-line metamaterials, there is clearly a need to develop three-dimensional structures that could be used more or less as volumetric "material" blocks instead of planar circuits.

The approach chosen in this thesis is to extend the well-known one- and two-dimensional transmission-line networks into three-dimensional structures. This requires the analysis of the propagation and impedance properties, as well as innovations in the manufacturing of such structures. For using these structures in applications where the sources of electromagnetic field are not integrated in the networks, a method of coupling the designed networks to free space or any other homogeneous medium is developed. Some of these results have been obtained in the Master's Thesis of the author [89], and these concepts and ideas are further developed here.

Although the three-dimensional transmission-line networks studied in this thesis can be designed to be effectively isotropic for the waves of voltages and currents, it is essential to note that they cannot support waves of any polarization. The wave propagation in the networks is studied for the fundamental mode of the transmission lines comprising the network and therefore the "wave polarization" is defined entirely by the transmission-line topology. When a transmission-line network is coupled with a homogeneous medium such as free space, the polarization of the wave impinging on the network must be defined. The coupling mechanism introduced in this thesis is shown to be able to couple linearly polarized waves (with TE-incidence) between the studied networks and a homogeneous medium.

The results presented in this chapter have been published in [**I**–**V**]. In addition, the author has contributed to several other papers related to this field of research [90–96].

4.2 Design principles

4.2.1 Dispersion equations

The basis of the analysis of the transmission-line networks studied in this thesis is the knowledge of propagation properties of waves that can travel inside the networks. In practice these propagation properties can be defined by equations for dispersion, i.e., the dependence of the wavenumber on the frequency, and by the dependence of the characteristic impedance of the network on the frequency. The design of three-dimensional networks therefore requires the generalization of the equations derived for one- and two-dimensional networks. A three-dimensional generalization of the unit cell of Fig. 3.1b is presented in [**I**]. The dispersion equation for such a network with periodic loads $Z_{\mathrm{load}} = 1/j\omega C$ and $Y_{\mathrm{load}} = 1/j\omega L$, where C is the capacitance and L the inductance, is found to be [**I**]

$$\cos(k_x d) + \cos(k_y d) + \cos(k_z d) = \frac{1}{2j\omega L S_{\mathrm{BW}}} - 3\frac{K_{\mathrm{BW}}}{S_{\mathrm{BW}}}, \tag{4.1}$$

where

$$S_{\mathrm{BW}} = \frac{j\omega C}{(D_{\mathrm{TL}} + j\omega C B_{\mathrm{TL}})(A_{\mathrm{TL}} + j\omega C B_{\mathrm{TL}}) + \omega^2 C^2 B_{\mathrm{TL}}^2}, \tag{4.2}$$

$$K_{\mathrm{BW}} = \frac{-(B_{\mathrm{TL}}C_{\mathrm{TL}} - D_{\mathrm{TL}}A_{\mathrm{TL}})(A_{\mathrm{TL}} + j\omega C B_{\mathrm{TL}})}{[(D_{\mathrm{TL}} + j\omega C B_{\mathrm{TL}})(A_{\mathrm{TL}} + j\omega C B_{\mathrm{TL}}) + \omega^2 C^2 B_{\mathrm{TL}}^2]B_{\mathrm{TL}}} - \frac{A_{\mathrm{TL}}}{B_{\mathrm{TL}}}. \tag{4.3}$$

In (4.1)–(4.3) K_{BW} and S_{BW} are functions depending on the propagation constant and characteristic impedance of the host transmission lines and on the capacitance of the loading capacitors. Here the host transmission line properties are represented by the ABCD-parameters (A_{TL}, B_{TL}, C_{TL}, D_{TL}) of a section of the host transmission line having the length $d/2$ [49]:

$$\begin{bmatrix} A_{\mathrm{TL}} & B_{\mathrm{TL}} \\ C_{\mathrm{TL}} & D_{\mathrm{TL}} \end{bmatrix} = \begin{bmatrix} \cos(k_{\mathrm{TL}} d/2) & jZ_{\mathrm{TL}} \sin(k_{\mathrm{TL}} d/2) \\ jZ_{\mathrm{TL}}^{-1} \sin(k_{\mathrm{TL}} d/2) & \cos(k_{\mathrm{TL}} d/2) \end{bmatrix}, \tag{4.4}$$

where k_{TL} and Z_{TL} are the wavenumber and characteristic impedance of a single section of the transmission line. In the case of lossy host transmission lines, the hyperbolic cosine and sine functions can be used, see eq. (10) in [**III**].

Equation (4.1) can be easily generalized for arbitrary loads Z_{load} and Y_{load} [**VI**]:

$$\cos(k_x d) + \cos(k_y d) + \cos(k_z d) = \frac{Y_{\mathrm{load}}}{2S} - 3\frac{K}{S}, \tag{4.5}$$

where

$$S = \frac{Z_{\mathrm{load}}}{(Z_{\mathrm{load}} A_{\mathrm{TL}} + B_{\mathrm{TL}})(Z_{\mathrm{load}} D_{\mathrm{TL}} + B_{\mathrm{TL}}) - B_{\mathrm{TL}}^2}, \tag{4.6}$$

$$K = \frac{Z_{\text{load}}(A_{\text{TL}}D_{\text{TL}} - B_{\text{TL}}C_{\text{TL}})(Z_{\text{load}}A_{\text{TL}} + B_{\text{TL}})}{[(Z_{\text{load}}A_{\text{TL}} + B_{\text{TL}})(Z_{\text{load}}D_{\text{TL}} + B_{\text{TL}}) - B_{\text{TL}}^2]B_{\text{TL}}} - \frac{A_{\text{TL}}}{B_{\text{TL}}}. \tag{4.7}$$

For unloaded networks equation (4.5) can be applied directly by inserting $Z_{\text{load}} \to 0$ and $Y_{\text{load}} \to 0$ [**I**,**VI**]. One- and two-dimensional loaded and unloaded networks can be analyzed with these equations simply by removing one or two of the cosine terms on the left side of equations (4.1) or (4.5), and by replacing the factor 3 on the right side of these equations with the factor 2 or with the factor 1, in the case of two-dimensional and one-dimensional networks, respectively.

4.2.2 Equations for impedance

Equations for the characteristic impedance (Bloch impedance) of the capacitively and inductively loaded, as well as for the unloaded three-dimensional networks, are derived in [**I**]. The characteristic impedance is defined at the ports of a three-dimensional extension of the unit cell of Fig. 3.1b as defined by (3.4). In the case of a three-dimensional capacitively and inductively loaded transmission-line network, the expression for the impedance is quite lengthy, so it is not repeated here. The reader is encouraged to peruse equation (25) in [**I**]. For any other type of periodic loading, i.e., for arbitrary Z_{load} and Y_{load}, the derivations in [**I**] can be easily repeated. An expression for the impedance in this general case can thus be derived from equation (25) in [**I**], and it reads

$$Z = \frac{Z_{\text{TL}} \tan\left(\frac{k_{\text{TL}}d}{2}\right) - j\frac{Z_{\text{load}}}{2}}{\tan\left(\frac{kd}{2}\right)}, \tag{4.8}$$

where $k = \sqrt{k_x^2 + k_y^2 + k_z^2}$ is the wavenumber in the network.

The characteristic impedance of an unloaded transmission-line network can be derived from (4.8) by inserting $Z_{\text{load}} \to 0$:

$$Z = Z_{\text{TL}} \frac{\tan\left(\frac{k_{\text{TL}}d}{2}\right)}{\tan\left(\frac{kd}{2}\right)}. \tag{4.9}$$

It must be noted that the characteristic impedance of the network depends on the wavenumber of the wave propagating in that network. Therefore, the impedance can be different for various propagation directions, since the wave vector $\overline{k}$ can have all three components k_x, k_y, and k_z nonzero. The analysis of the characteristic impedance is simplified by the fact that it is similarly isotropic as the wavenumber. It is also worth noting that (4.8) and (4.9) can be applied as such in analysis of one-dimensional and two-dimensional networks.

4.2.3 Coupling of transmission-line networks with homogeneous media

Another design issue is related to the coupling of waves between a transmission-line network and a (homogeneous) medium, such as free space, surrounding this network. In [**IV**,**V**] this coupling has been achieved by using a special transition layer between the network and the surrounding free space. This layer is basically an extension of the open transmission lines at the edges of the network: by gradually extending parallel-strip transmission lines connected to these edges we can effectively cover the whole interface between a slab composed of the transmission-line network and the medium surrounding this slab.

In the case of realizable transmission-line networks, especially those supporting backward-wave propagation, it may be impossible to achieve the optimal characteristic impedance of the network in a wide frequency band due to the inevitable dispersion [1–3]. However, the non-resonant (and thus relatively wide-band) coupling method based on the use of the transition layer described above is shown to be able to couple the electromagnetic fields between a transmission-line network and the surrounding free space in a wide frequency band even with taking into account the mismatch in the impedances [**IV**,**V**].

4.3 Analytical and numerical results

The analytical expressions for the dispersion in a three-dimensional backward-wave transmission-line network, i.e., equation (4.1) and the similar expression for the forward-wave case where the load impedance Z_{load} and admittance Y_{load} tend to zero, are verified in [**III**] with numerical simulations of a realizable structure in which the host network is composed of microstrip transmission lines, as shown in Fig. 4.1. The capacitive and inductive loads are modelled as lumped elements with sizes and parameters comparable to those of commercially available surface-mounted components.

The agreement between analytical and numerical results is very good, verifying the usability of equations (4.1)–(4.7) for accurate design of practically realizable structures. See Fig. 4.2 for the analytical and numerical results of the dispersion in forward-wave and backward-wave networks as those in Fig. 4.1, calculated for the axial propagation in the networks. Figs. 4 and 5 in [**III**] give further confirmation on the effective isotropy of these networks since the dispersion curves of different propagation directions are overlapping in the frequency region where the structures are designed to operate. The isotropy is essentially due to the electrically short period of the networks. Here it must be noted that instead of the free-space wavelength, the effective wavelength inside the structures should be used as a measure of electrical length of a single period.

In paper [**III**] the resolution enhancement capability of a slab composed of the pro-

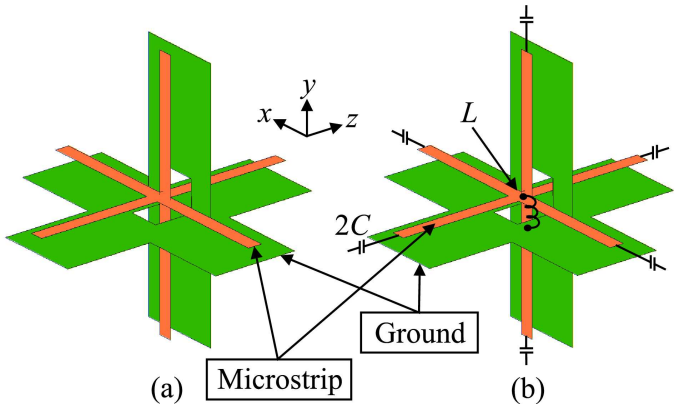

Figure 4.1: From [**III**]. Unit cells of three-dimensional forward-wave (a) and backward-wave (b) transmission-line networks based on the microstrip technology (the substrate is not shown for clarity).

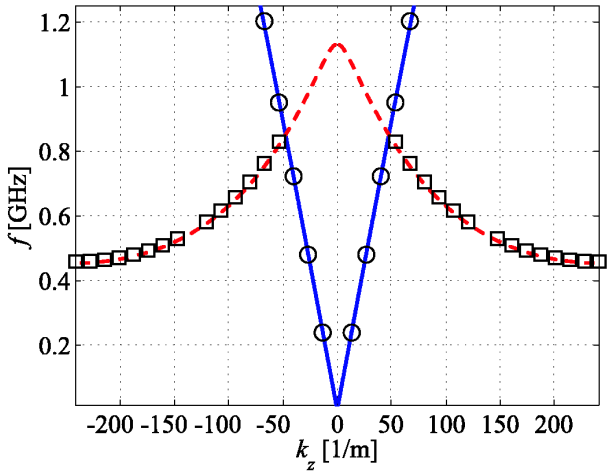

Figure 4.2: From [**III**]. Dispersion curves for the forward-wave (solid line: analytical; circles: HFSS) and backward-wave (dashed line: analytical; squares: HFSS) networks. Propagation along the z-axis is considered ($k_x = k_y = 0$).

posed three-dimensional transmission-line network is studied. This is done by using the equations describing the transmission through a finite-thickness slab composed of such a network, see equations (42) and (43) in [**I**]. Here the backward-wave slab is sandwiched between two half-spaces composed of a three-dimensional forward-wave network where the source and image planes are situated. Even when taking into account realistic losses in the studied structure, it is shown that sub-wavelength

resolution is possible for slabs of reasonable thickness. Fig. 4.3 presents the dependence of the resolution enhancement (R_e) of the designed backward-wave slab on the slab thickness l [**III**]. The source and image planes are situated at distance $l/2$ away from the slab edges, which results in a source-to-image distance of $2l$.

R_e describes what is the resolution enhancement offered by the slab, as compared to any conventional, diffraction-limited lens. This parameter is simply the ratio of the maximum transverse wavenumber which is recovered in the image plane, and the wavenumber corresponding to propagating modes, i.e.,

$$R_\mathrm{e} = \frac{k_{t,\mathrm{max}}}{k_\mathrm{eff}}. \tag{4.10}$$

It should be noted that here k_eff denotes the effective wavenumber in the network, not in free space. Obviously, for any lens that can recover some part of the evanescent spectrum ($k_t > k_\mathrm{eff}$), the resolution enhancement will be larger than one. As illustrated by Fig. 4.3, the resolution enhancement quickly approaches the value 1 as the source-to-image distance and the lens thickness are increased. This is an expected consequence of losses, the effect of which rapidly grows stronger as the lens thickness is increased. From these results it can be concluded that a resolution enhancement of $R_\mathrm{e} = 2$ is obtainable with a source-to-image distance of about a wavelength.

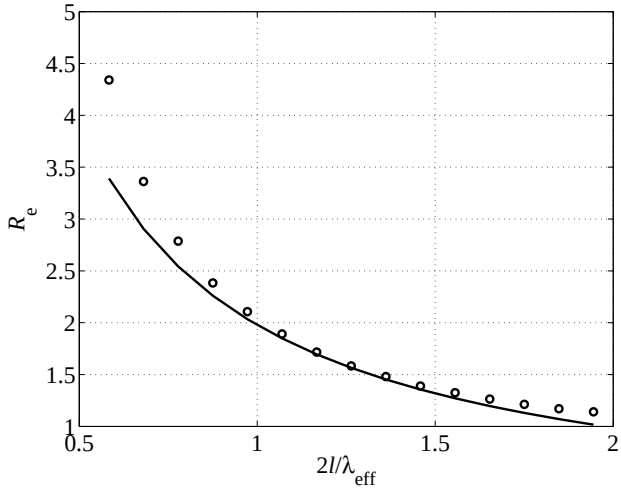

Figure 4.3: From [**III**]. Resolution enhancement of the studied lens, as a function of the distance between source and image (in wavelengths at the optimal operation frequency, $f = 0.8513$ GHz). Circles: R_e calculated from the transmission coefficient data. Solid line: approximation for R_e, calculated using the equation from [64].

In papers [**I**–**III**] the backward-wave networks are placed between two half-spaces composed of a forward-wave network. This enables easy analysis of the backward-wave slabs since the forward-wave and backward-wave networks are coupled well to

each other simply by connecting the transmission lines of these networks. For practical applications, however, the situation is more complicated, since any backward-wave slab composed of a network as studied here is not well coupled to homogeneous media, such as free space. To enable coupling of waves between the proposed type of backward-wave network and a homogeneous medium, a coupling method based on parallel-strip transmission lines is proposed in [**IV**]. The coupling between the network and free space surrounding it are studied with full-wave simulations by illuminating a transversally infinite slab composed of this network with plane waves incident from free space. The dispersion characteristics and impedance of the backward-wave network are designed so that the effective refractive index equals approximately $n \approx -1$ and the impedance $Z \approx 377\ \Omega$ at the frequency of 4 GHz.

See Fig. 4.4 for the simulation model of the slab and the simulated reflection and transmission coefficients as functions of the frequency (for the normal incidence). The simulation results presented here and in [**IV**] confirm good coupling of waves between the slab and free space for a wide range of incidence angles in the xz-plane (TE-polarization, electric field parallel to the y-axis) and also the negative refraction occurring at the interfaces between the slab and free space.

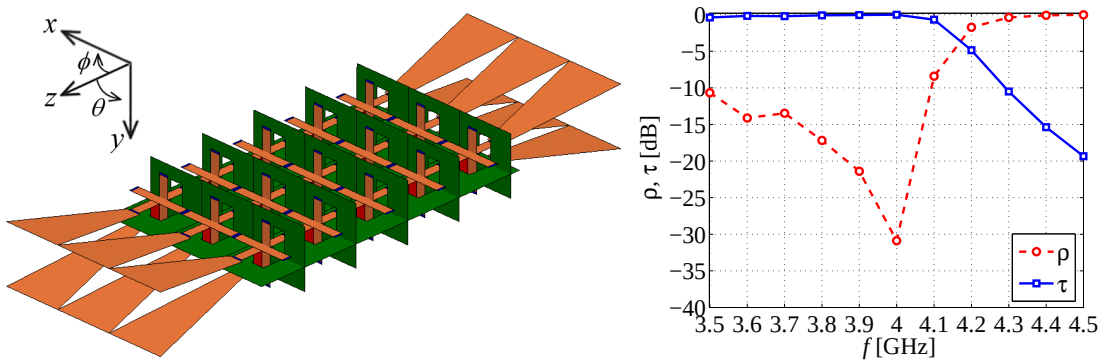

(a) (b)

Figure 4.4: (a) From [**V**]. Simulation model of the backward-wave slab studied in [**IV**,**V**]. The slab is periodically infinite in the x- and y-directions. Three unit cells are modelled along the x-direction for the visualization of wave refraction. (b) From [**IV**]. Simulated reflection and transmission through the backward-wave slab as a function of frequency for the normal incidence.

The study of the backward-wave slab introduced in [**IV**] is continued in [**V**] by analyzing and simulating the electrical tunability of the refractive index in this slab. In practice such tunability can be achieved by replacing the lumped capacitors loading the network by varactors. The effect of the tuning of the refractive index and the impedance are studied both analytically and numerically. Good coupling of electromagnetic waves for different incidence angles in both xz- and yz-planes (see Fig. 4.4a), as well as for different refractive indices is confirmed by simulating plane wave reflection and transmission in the studied slab while tuning the value of the lumped capacitances [**V**].

4.4 Realization

The proposed circuit topology of three-dimensional transmission-line networks analyzed in [**I**] can be realized in principle with many types of transmission lines. For practical realizations, transmission lines based on the microstrip technology have been found to be feasible. Such structures, with unit cells similar to the ones of Fig. 4.1, are studied analytically and numerically in [**I**–**III**]. An experimental demonstration of this type of a structure, based on connecting stacked two-dimensional networks of microstrip transmission lines with each other by vertical sections of similar lines, is presented in [**II**].

The manufacturing of this three-dimensional transmission-line network is possible with standard etching equipment and the assembly can be done in normal laboratory conditions by soldering the different layers together. The lumped capacitive and inductive elements are realized as surface mounted components. See Fig. 4.5 for a photograph of the realized structure composed of three horizontal layers connected to each other by vertical microstrips. The resulting structure is isotropic with respect to the waves of voltages and currents travelling inside the network. The backward-wave propagation in the part of the structure which is loaded by the lumped capacitors and inductors, as well as the existence of strong evanescent fields at the second interface between the forward-wave and backward-wave networks, are confirmed with measurements [**II**].

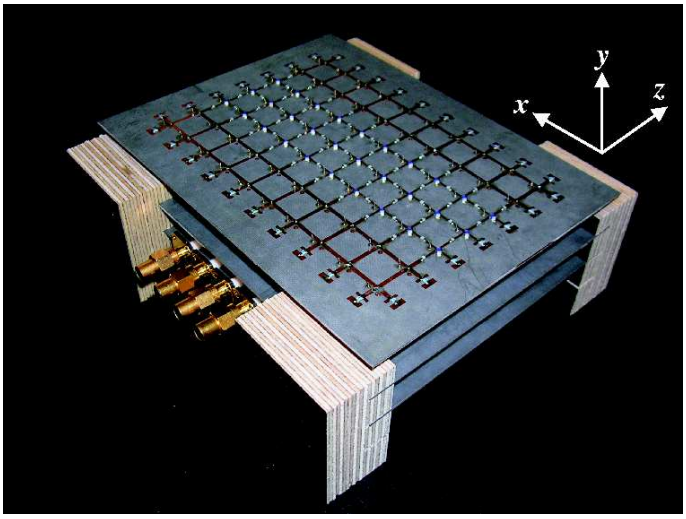

Figure 4.5: From [**II**]. Experimental prototype of a structure composed of three-dimensional forward-wave and backward-wave transmission-line networks.

4.5 Review of related results found in the literature

Here we briefly review the results found in the literature that are essentially related to the topic of this chapter. First, we review some papers that discuss various ways of analyzing and creating three-dimensional backward-wave media based on loaded transmission-line networks. Also the coupling of these and other types of transmission-line networks with free space are considered. Finally, we present some alternative methods for obtaining sub-wavelength resolution that do not require the use of any type of backward-wave media.

4.5.1 Various types of loaded transmission-line networks

Various one- and two-dimensional loaded and unloaded transmission-line networks have been reported and studied for example in [2, 3, 51–67]. Here we briefly review results found in the literature that are more related to the topic of this chapter, i.e. three-dimensional transmission-line networks and coupling of such networks with free space.

Paper [97] presents circuit topology of a three-dimensional loaded transmission-line network. The unit cell design is based on the transmission-line matrix (TLM) method. There are two orthogonally oriented transmission lines on each face of a cubic unit cell. As these lines can be periodically loaded with capacitances and inductances, backward-wave propagation in this isotropic network is possible. Note that this network is fully isotropic, i.e., it can support waves of any polarization, whereas the three-dimensional networks studied in [**I**-**V**] are isotropic only for waves of voltages and currents. As a natural consequence, the topology proposed in [97] is much more difficult to realize. It is also worth noting that the designed network can be coupled with free space as such, and this coupling is confirmed for normal incidence with numerical simulations [97]. Paper [98] presents a realizable unit cell of a structure similar to the one presented in [97]. Backward-wave propagation in the structure as well as coupling with free space are demonstrated with numerical simulations.

In [99] a three-dimensional transmission-line network topology, composed of parallel strip transmission lines and lumped capacitive and inductive loads, is presented. A backward-wave network based on such a design is studied numerically.

In [100] yet another topology of three-dimensional backward-wave transmission-line networks is presented. Also this network is in principle fully isotropic, i.e., it supports waves of all possible polarizations. Again, the realizability of such a network is demanding. In [100] one unit cell of the proposed network is manufactured and measured.

Two-dimensional loaded transmission-line networks exhibiting backward-wave propagation are much easier to realize than their three-dimensional counterparts. Vol-

umetric structures composed of two-dimensional networks that are coupled with free space have been recently reported [101–104]. With such networks, experimental proof of sub-wavelength imaging of sources placed in free space have also been provided [103, 104].

4.5.2 Alternative methods for sub-wavelength imaging

This chapter has concentrated on the topic of realization of backward-wave media with volumetric transmission-line networks. Backward-wave media composed of resonant particles such as split-ring resonators and wires were discussed in Chapter 2. Imaging with sub-wavelength resolution can be obtained also with various other methods besides using backward-wave media. As explained in Chapter 2, the essential phenomenon enabling sub-wavelength resolution is the amplification of evanescent waves. This can be achieved without a backward-wave medium by creating such conditions that at certain surfaces or interfaces, similar surface plasmons are excited, as would be excited at an interface between a forward-wave and a backward-wave medium [105]. Such surface plasmons can be excited for example in arrays of resonant particles [90–92, 105–107], or, for example, at the surface of silver [108].

It is also possible to "channel" electromagnetic fields with sub-wavelength resolution by creating a medium in which the evanescent modes are transformed into propagating modes. This technique, with which an "image" of the source field can be transmitted far away from the source, has been studied widely in the recent literature, see, e.g., [109–115].

Recently the concepts of near-field focusing screens and plates have been proposed [116–119]. These devices are based on grating-like structures, i.e., they are simply metallic screens or plates that have part of the metal removed to form a certain pattern in them. Such structures are shown to be able to focus electromagnetic waves into focal spots of sub-wavelength size.

4.6 Summary of related publications

In paper [**I**] we present the idea of extending the analysis of one- and two-dimensional unloaded and loaded transmission-line networks into three dimensions. The basic design equations, i.e., equations for wavenumbers and characteristic impedances in the both types of networks are derived. Dispersion and impedance characteristics of loaded and unloaded three-dimensional transmission-line networks are studied and discussed. Two types of realizable host transmission-line networks are presented. Results of numerical simulations of a three-dimensional transmission-line structure, based on the microstrip technology, are given.

Paper [**II**] presents an experimental prototype of a structure comprising three-dimensional transmission-line networks, exhibiting forward and backward-wave propagation characteristics. Losses inside the networks are studied analytically and equations for evaluating the losses are given. Transmission properties of a slab composed of a transmission-line network with realistic losses are studied. Expected type of wave propagation in the structure is confirmed with measurements.

Paper [**III**] discusses the isotropy of wave propagation in three-dimensional transmission-line networks. It is confirmed, both analytically and numerically, that in the proposed types of three-dimensional loaded and unloaded networks, wave propagation is isotropic in certain frequency regions, where the network period is electrically sufficiently small. The resolution characteristics of a slab composed of a three-dimensional loaded transmission-line network are studied. It is concluded that sub-wavelength resolution is possible even when taking into account realistic losses in the structure.

A way of coupling electromagnetic fields between a backward-wave transmission-line network and a homogeneous medium surrounding this network is proposed in [**IV**]. This coupling method includes a layer of gradually enlarging transmission lines that act as mode transformers between the network and the surrounding free space. The operation of the proposed coupling method is confirmed with numerical simulations of a slab composed of a transmission-line network placed in free space.

Paper [**V**] is based on the same design as presented in [**IV**]. Here the capacitance of the lumped series capacitors is varied in order to obtain an electrically tunable index of refraction. In practice this tuning can be done, e.g., by using varactors. The analytical equations used to design the slab are given further confirmation by evaluating the effective inductance and capacitance of the lumped elements inserted in the simulation model. These effective values are shown to correspond well to the analytically derived optimal values. The method of coupling electromagnetic fields between the slab and the surrounding free space is shown to be efficient even though the impedance of the slab is tuned away from the optimal value.

5 Electromagnetic cloaking with volumetric structures composed of transmission-line networks

5.1 Introduction

Within this thesis the term "cloaking" refers to the reduction of an object's total scattering cross section. This means that the scattering cross section of the object should be reduced for electromagnetic waves with any angle of incidence and for any position of the observer in the far-field. Also the near-fields around the object should not be disturbed by the object or the cloak. For cloaks that are periodic along one axis, such as the ones studied in this thesis, the angle of incidence varies only in the plane orthogonal to the structure axis. Cloaking differs from other scattering reduction methods in that it enables reduction of scattering cross section in all directions, including forward scattering. Therefore some other techniques that are used for scattering reduction, such as the stealth technology, do not meet the requirements of cloaking in this sense. Cloaking can be achieved in many ways. During the recent years, especially two such methods, namely, the scattering cancellation technique [33] and the coordinate transformation technique [34, 35], have gained a wide interest in the scientific community. In this thesis, we propose an alternative cloaking technique, which is based on the use of transmission-line networks that are coupled with the homogeneous media surrounding these networks. Also the two cloaking methods mentioned above are briefly reviewed in this chapter and references to other techniques are given.

The results presented in this chapter have been published in [**VI**–**X**]. In addition, the author has contributed to several other papers related to this field of research [42, 120–125].

5.2 Design principles

Cloaking with networks of transmission lines is based on the following principle: in order to minimize scattering, a cloak device consists of a "medium" which behaves as the medium surrounding it, while having the possibility of squeezing fields inside certain sections of the cloak, creating a space inside the cloak where electromagnetic fields are not coupled into. This type of cloak medium can be illustrated as a transmission-line network into which the impinging electromagnetic fields are coupled to, and inside which, there is space where electromagnetic waves do not enter. Since, in the ideal case, all the fields are confined inside the transmission lines, the space which is left "cloaked" is obviously the space between the adjacent sections of transmission lines. See Fig. 5.1 for an illustration of the cloaking principle in the case of a two-dimensional network. This type of cloak can be made volumetric by stacking adjacent two-dimensional networks on top of each other.

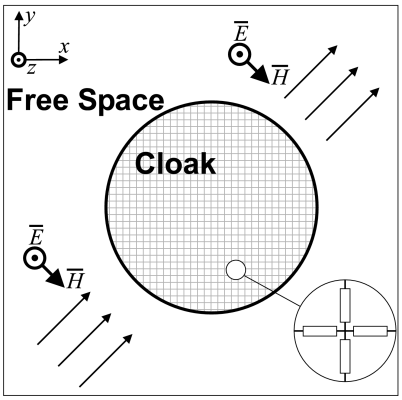

Figure 5.1: From [**VI**], [126]. A two-dimensional cylindrical electromagnetic cloak. The cloak operation does not depend on the incidence angle of the illuminating electromagnetic wave, as long as the network period is small enough with respect to the wavelength.

Although the cloak depicted in Fig. 5.1 is cylindrical, this cloaking method is not restricted to cylindrical or spherical shapes. The cloak can naturally be of any shape, since the fields are just guided through the structure. But, for practical reasons and due to the necessary existence of small scattering, the cloak needs to be cylindrical in the two-dimensional case and spherical in the three-dimensional case in order to behave in a similar way for waves impinging on the cloak from different directions. This symmetry helps in the analysis of the cloak properties, since the cloak can be assumed to operate in a similar way regardless of the incidence angle. Therefore, simulations and measurements need to be conducted in principle for only one incidence angle in order to find out the structure's cloaking capabilities.

For cloaking of objects in free space with the transmission-line technique, there is a limitation: inside the cloak network, the waves cannot propagate with the speed of light, as they do in free space, even though the material filling the transmission lines would be vacuum [**VI**]. The geometry of the network itself slows down the electromagnetic waves, resulting in a wavenumber k_{eff} that is larger than the free-space wavenumber k_0 by a factor of $\sqrt{2}$ or $\sqrt{3}$, in the cases of a two-dimensional network and a three-dimensional network, respectively. This slowing down is due to the fact that even though in a single transmission-line section the wave propagates with the wavenumber k_0 (assuming that the material filling this transmission line is vacuum), this single transmission line "sees" the other transmission lines of the network as periodical loads, thus changing the effective wavenumber of the wave travelling in this network. This periodical loading is naturally more significant for a three-dimensional network than for a two-dimensional one, hence the difference in the factor of increase in the effective wavenumber.

The non-ideality of the wavenumber, i.e., the speed with which the wave propagates inside the cloak network, results in that this type of cloak will necessarily scatter. The interesting question is that how significant this scattering is, and if it can be somehow compensated. In this thesis work, it has been found that for electrically small cloaks, with the diameter considerably smaller than the wavelength of the impinging electromagnetic radiation, the cloaking performance is very good even with the non-ideal wavenumber. Also for electrically large cloaks, with the diameter larger than the wavelength of the impinging electromagnetic radiation, the cloaking effect can be obtained, but only in a much smaller frequency band than with smaller cloaks.

One way to compensate for the increase in the wavenumber would be to periodically load the transmission-line networks with loads that cancel the undesired slowing down of the wave. This can be achieved with a similar type of loading as used in the creation of backward-wave networks, i.e., increase of the series capacitance and/or increase of the shunt inductance of the transmission lines [**VI**]. This compensation comes with a price: the bandwidth of cloaking will be unavoidably decreased since dispersion will be introduced into the frequency dependence of both the wavenumber and the characteristic impedance of the networks. This will also force the energy propagation velocity (group velocity) to be different from the phase propagation velocity, which are equal in the case of unloaded networks. In fact, the equality of phase and group velocities is a very unique feature inherent only to cloaks composed of unloaded transmission-line networks. This feature is an important benefit of this cloaking technique as compared to many other techniques.

Basic design guidelines for cloaks based on the transmission-line technique are the same as considered in Chapter 4: the proper choice of the dispersion (wavenumber) and the characteristic impedance. The study of the dispersion is required for the determination of the cloak period, which defines the frequency range where isotropy of the propagation is achieved. The study of the characteristic impedance in principle enables design of the transmission line dimensions in such a way that optimal impedance matching with the medium surrounding the cloak can be achieved in the desired frequency range. Another design issue is the coupling of waves between a transmission-line network and the medium surrounding this network. In [**VI**–**X**] this coupling has been achieved by using a special transition layer between the network and the surrounding free space. As described in Chapter 4, this layer can be realized by extending the transmission lines at the edge of the cloak, effectively covering the whole interface between the cloak and the surrounding medium.

For many types of transmission lines, such as microstrips or parallel-strip transmission lines as used here, it may be impossible to achieve the optimal characteristic impedance of the network since this usually requires very large values of the impedance of single sections of transmission lines [**VI**]. As discovered for a backward-wave slab [**IV**,**V**] and for various cloaking structures [**VI**–**X**], the impedance mismatch between such networks and the surrounding medium can be effectively mitigated by the use of the proposed type of transition layer.

The most significant limitation of the transmission-line technique in cloaking applications is the cloaked object's geometry: the object must fit between the adjacent sections of transmission lines and therefore it cannot be, e.g., an electrically large solid cylinder or a sphere. In papers [**VI**–**VIII**] the cloaked objects are composed of periodic two-dimensional arrays of metal cylinders having a small diameter and, effectively, infinite in height. In papers [**IX**,**X**] it is demonstrated that the same cloaking technique can be applied also to cloaking of more complicated three-dimensional objects. Another limitation is that with the proposed coupling method the transmission-line networks and the homogeneous media surrounding them can in principle be well coupled only for a single (linear) polarization at a time, depending on the geometry of the transition layer.

5.3 Numerical results

The cloaking effect of an idealized two-dimensional transmission-line cloak is studied in [**VI**], where the cloak, placed in free space, is modelled as a homogeneous material having a cylindrical shape and the material parameters equal to $\varepsilon_\mathrm{r} = \mu_\mathrm{r} = \sqrt{2}$, which result in the same wavenumber as a two-dimensional transmission-line network (with vacuum filling the transmission lines) would have. This type of simulation assumes perfect coupling of waves, i.e., perfect impedance matching, between the cloak and the surrounding medium. The results confirm that although some forward scattering inevitably occurs, at the frequencies where the cloak diameter is small compared to the wavelength, cloaking is very effective. Also it is found that there are frequency regions inside which cloaking is possible also with cloaks having electrically large diameters [**VI**]. This effect is concluded to be a result of the matching of wave fronts of waves travelling inside and outside the cloak. Thus, cloaking with electrically large cloaks is obtainable at frequencies where the wave inside the cloak travels a distance which differs from the distance travelled in the surrounding medium by a multiple of the wavelength.

Coupling of electromagnetic waves between realizable transmission-line networks and the free space surrounding these structures, is studied numerically in [**VI**,**VII**]. In these cases the network has either a rectangular or a square shape, which does not enable "cloaking" in the sense that the total scattering cross sections of objects placed inside these structures would be reduced. Instead, the goal is to study the coupling phenomenon as such, which then enables design of cloaking devices in which the network itself is designed with the point of view of the reduction of the total scattering cross section. It must be noted though, that structures as studied in [**VI**,**VII**] may be used in other applications. For example, such structures could be used as walls or slabs which let only certain frequencies through them and therefore act as kind of filters.

A design of a cylindrical cloak, based on the transmission-line technique proposed in this thesis, is presented in [**VIII**]. Here the transmission-line network is designed

so that it has a cylindrical shape and its unit cell size is small as compared to the wavelength, in order to achieve isotropic propagation in the network. Also, the diameter of the cloak network is made smaller than approximately half wavelength at the desired operation frequency. The transition layer proposed and studied in [**VI**,**VII**] is used in the cylindrical cloak by placing the transmission lines of the transition layer radially around the cloak. The dimensions of the cloak are optimized with numerical simulations to obtain a wide-band cloaking effect with the center frequency around 3 GHz. The total scattering cross sections of cloaked and uncloaked arrays of perfectly conducting rods are simulated and results show that an efficient cloaking effect indeed occurs, and in a relatively wide frequency band. See Fig. 5.2a for the cloak dimensions. The wide-band and isotropic cloaking effect is confirmed with numerical simulations, as demonstrated by the results shown in Figs. 5.2b and 5.2c.

In [**IX**] the study of the cloak shown in Fig. 5.2a is continued. The cloaking effect is further verified by studying the electric field distributions in simulation models with and without the cloak, see Fig. 5.3. Also the effects of changing the transition layer thickness and the impedance of the transmission lines composing the network itself are studied in [**IX**]. The results indicate that the thickness of the transition layer can be effectively used to control the frequency response of the cloak, whereas moderate changes in the impedance of the network do not affect significantly on the optimal cloaking frequency or bandwidth.

Paper [**X**] presents a study of a cylindrical cloak with the diameter equal to several wavelengths at the operation frequency. The structure of this cloak is similar to the one presented in [**VIII**], but the cloak is made larger by increasing the number of unit cells in the network comprising the cloak. Based on numerical simulations, the resulting cloaking effect is more narrowband as compared to electrically small cloaks, as expected. Nevertheless, the results in [**X**] demonstrate the potential in cloaking of electrically large objects with the transmission-line method.

In [**X**] also the operation of the electrically small cloak presented in [**VIII**] is studied. In this study the cloak is used to reduce the scattering from a metallic object situated close to a dipole antenna. The goal is to study the cloaking performance in a realistic scenario where the electromagnetic wave impinging on the cloak is not an ideal plane wave. Since the cloak is placed very close to the dipole, the waves impinge on the cloak with various incidence angles in both E- and H-planes. Numerical simulations demonstrate that the directivity pattern of the dipole is changed considerably when the uncloaked object is placed close to it, whereas with the cloaked object the directivity pattern is similar to the case of the dipole alone in free space [**X**].

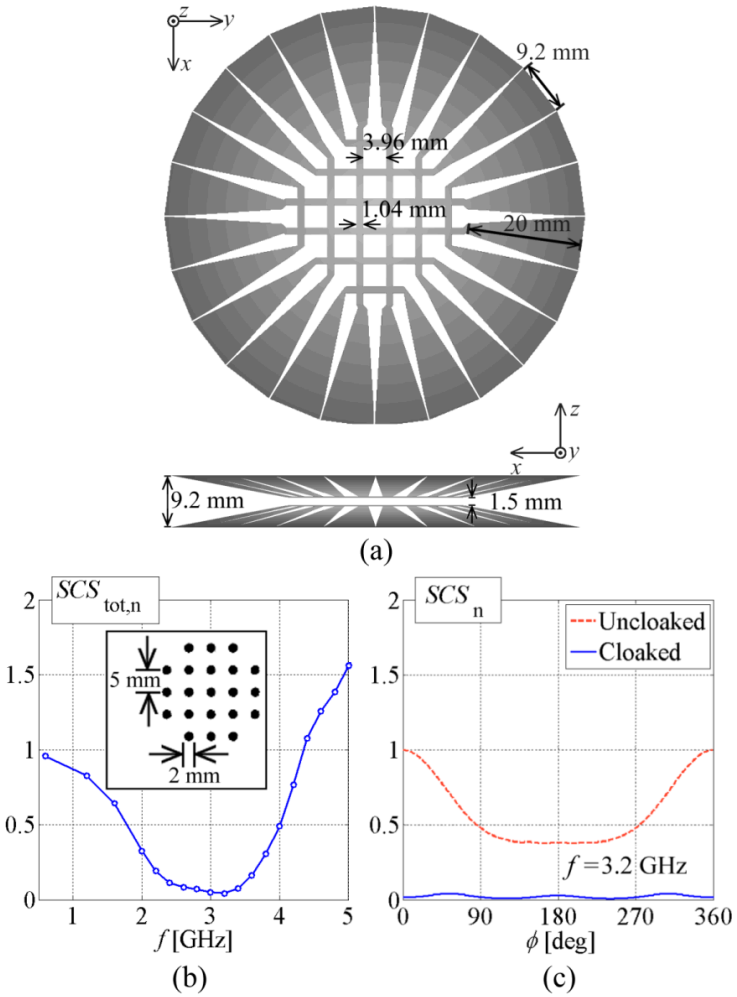

Figure 5.2: From [**VIII**]. (a) Cloak structure and dimensions in the xy-plane (top) and in the xz-plane (bottom). (b) Full-wave simulated total SCS of the cloaked object, normalized to that of the uncloaked object. The inset shows the dimensions of the cloaked array of infinitely long metal rods in a xy-plane cut. (c) Full-wave simulated SCS of uncloaked and cloaked objects at the frequency of 3.2 GHz, normalized to the maximum SCS of the uncloaked object. ϕ is the angle in the xy-plane and the plane wave illuminating the cloak travels to the $+x$-direction, i.e., in the direction $\phi = 0$.

5.4 Experimental results

Measurements of a two-dimensional square-shaped transmission-line network are presented in [**VII**]. The network is placed inside a parallel-plate waveguide. Thus, the measurement setup emulates an effectively volumetric structure which is infinite in the vertical direction. Since the network has a square shape, it is not quite proper to call it a cloak. The purpose of the device is not the reduction of the

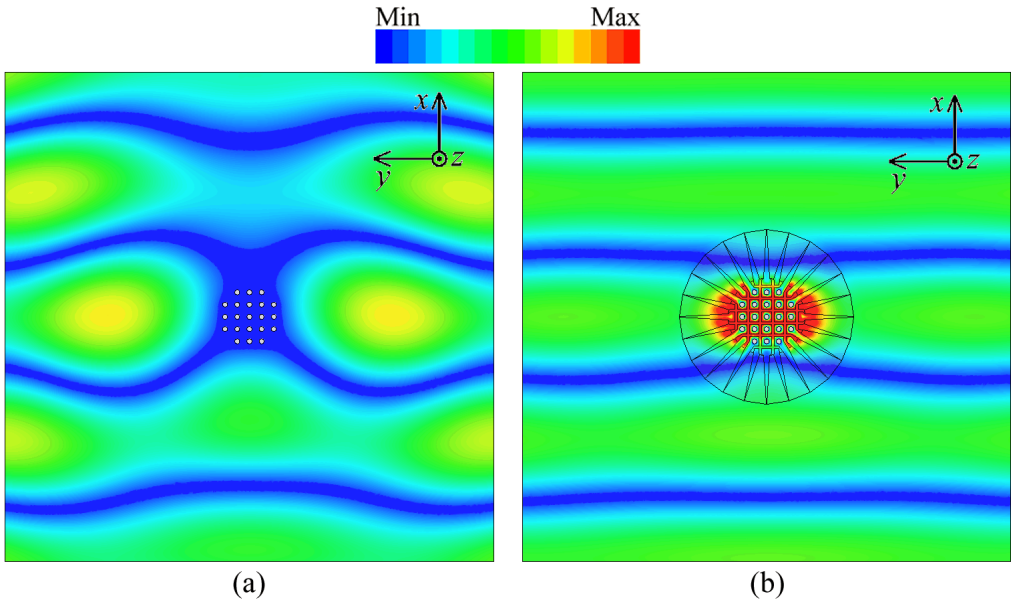

Figure 5.3: From [**IX**]. Full-wave simulated electric field distributions at the frequency 3 GHz for (a) uncloaked and (b) cloaked objects. The plane wave illuminating the structures travels in the $+x$-direction and has electric field parallel to the z-axis.

total scattering cross section, but the verification of the good coupling between the network and the surrounding free space. The potential of transmission-line networks in cloaking applications is demonstrated by the fact that the fields can propagate inside the network through an electrically dense array of metal objects, which alone is impenetrable to the impinging electromagnetic radiation.

A cylindrical wave is excited close to the network with a coaxial probe placed inside the waveguide. The electric field distributions inside the waveguide are measured with a vector network analyzer by measuring the transmission from the excitation probe to another probe that is placed outside the waveguide. A small fraction of the field inside the waveguide penetrates through the top wall of the waveguide since this wall is composed of a dense wire mesh. A scanner moving the waveguide under the stationary probe which is placed on top of the waveguide enables the measurements to be conducted for a large number of points in an efficient way. This measurement method was originally proposed in [90]. The results clearly show that the incident cylindrical wave is coupled into the network and travels inside the network coming out from the other side, with the array of metal rods inside the network. For comparison, the same measurement is repeated for an empty waveguide and for the array of metal rods without the network surrounding it. The results of the latter demonstrate that the array of metal rods is indeed impenetrable to the impinging electromagnetic radiation.

A realization of a volumetric cylindrical cloak with the same dimensions as shown in Fig. 5.2a is presented and measured in [**VIII**,**IX**]. The cloak comprises four sets of cylindrical networks that are stacked on top of each other. The cloak is used to "hide" an array of metal rods inside a rectangular waveguide. In principle a near-field measurement as the one conducted in [**VII**] is of course also possible. The problem with such measurements is that they do not provide any quantitative data on the cloaking performance and therefore the analysis of the cloaking effect is difficult with only measured field distributions. Also the waveguide measurement is somewhat limited because the total scattering cross section of an object placed inside the waveguide cannot be directly extracted from the measured reflection and transmission data. But because both the magnitude and phase information of transmission and reflection can be analyzed, we can have a very good understanding of how well the cloak operates by comparing the data between cloaked and uncloaked cases. Furthermore, the uncloaked and cloaked cases can be compared also to the transmission and reflection properties of an empty waveguide.

The results of these waveguide measurements are presented in Fig. 5.4, where the magnitude and phase of the transmission coefficient S_{21} are plotted as functions of the frequency. These results clearly demonstrate that the expected cloaking effect takes place in a wide frequency band, and especially in the frequency range around 3 GHz, where the transmission in the cloaked case corresponds very well to the situation in the empty waveguide, whereas the uncloaked object basically prevents any transmission through the waveguide. As can be seen from Fig. 5.4b, the phase of S_{21} in the cloaked case differs slightly from that in the empty waveguide. This is expected since the wavenumber inside the cloak is larger than in free space by a factor of $\sqrt{2}$. This effect "slows" the wave that travels inside the cloak and results in some scattering as has been previously discussed [**VI**]. This inevitable scattering, at least in the case of an electrically small cloak, does not prevent very good cloaking performance as can be concluded from Figs. 5.2b and 5.2c.

The same cloak and measurement waveguide as discussed above is used in [**IX**] to cloak a fully three-dimensional metal object. The cloaked object is in this case formed of a two-dimensional array of metal rods and of metal cylinders that are periodically connected to this array, as demonstrated in Fig. 5.5c. The results for the measured transmission magnitude and phase shown in Figs. 5.5a and 5.5b are almost the same as in the case of the two-dimensional array of rods. This is because the fields are confined inside the two-dimensional transmission-line networks and therefore in the volume between the adjacent networks (where the metal cylinders are placed) magnitudes of electromagnetic fields are effectively zero. The results presented in Fig. 5.5 confirm that the proposed cloaking method can indeed be used for cloaking three-dimensional objects, as long as these objects fit inside the mesh of transmission lines.

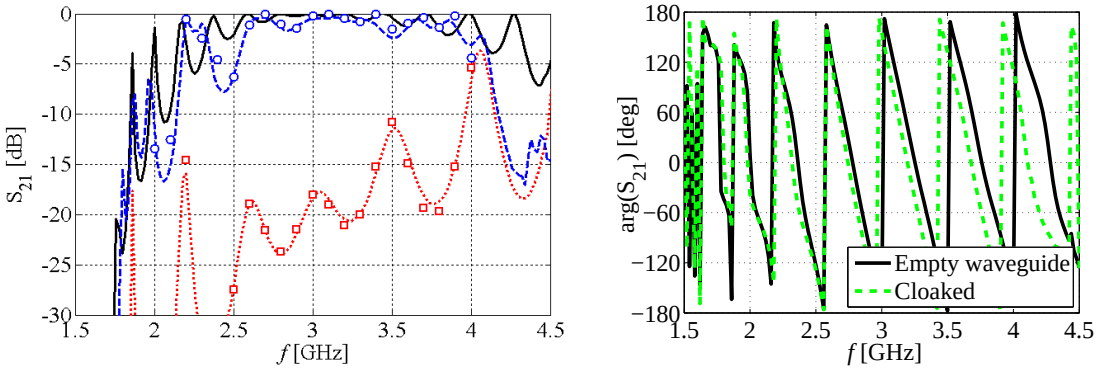

(a) (b)

Figure 5.4: (a) From [**VIII**]. Measured transmission magnitude for the empty waveguide (solid line), waveguide with the uncloaked object inside (dotted line) and waveguide with the cloaked object inside (dashed line). For comparison the full-wave simulated transmission corresponding to the uncloaked (squares) and cloaked (circles) cases are also shown. (b) From [**IX**]. Measured transmission phase for the empty waveguide and for the waveguide with the cloaked object inside.

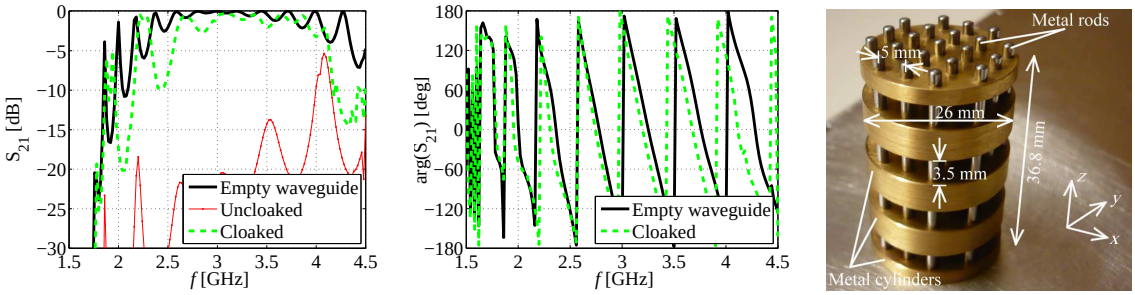

(a) (b) (c)

Figure 5.5: From [**IX**]. (a) Measured transmission magnitude. (b) Measured transmission phase. (c) Photograph of the object that is cloaked.

5.5 Review of related results found in the literature

5.5.1 Scattering cancellation technique

The principle of the scattering cancellation technique was introduced by Alù and Engheta in [33], although it must be noted that similar ideas were presented in the literature before [37, 38, 40]. The scattering cancellation approach is based on the following principle: an object, which we want to "hide" or "cloak", scatters because

the impinging electromagnetic field induces polarization in this object. Usually, for many simple objects such as spheres or cylinders, the dipolar scattering is the dominating one. If this object is then covered with another material, in which the polarization of opposite sign is induced, and furthermore, if the amounts of the induced polarizations are equal in the object and its cover, the total induced polarization is equal to zero. See Fig. 5.6 for an illustration of this principle.

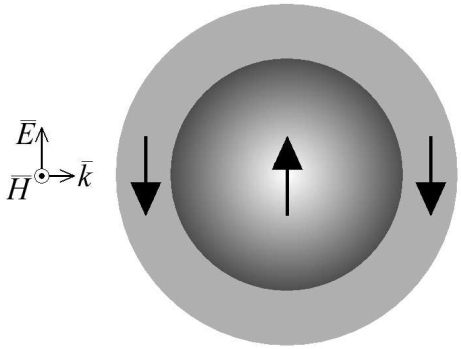

Figure 5.6: A spherical object, surrounded by a spherical shell, in which dipolar moments of the opposite sign are induced. If the amplitudes of the polarizabilities of the object and the shell are equal, the scattering from the system can be very small.

In principle the scattering cancellation technique can only be applied to the reduction of scattering from a known object, since the cover material and size should be designed based on the object which is placed inside the cover. How about cloaking of objects composed of an arbitrary material? This clearly requires that a certain volume of space is forced to have no electromagnetic fields inside. The scattering cancellation approach can be used also to design cloaks of this type. For example, the object that is cloaked can be a hollow metallic enclosure. This way any object of arbitrary material can be, in principle, placed inside this hollow enclosure inside which electromagnetic fields do not penetrate [41]. Naturally, the requirements for cloaking a conducting object are much more demanding than the ones needed to cloak, e.g., a dielectric object inside which electromagnetic fields are allowed to propagate.

The concept of cloaking with the scattering cancellation technique has been extensively studied in recent years [33,41,127–134]. The scattering cancellation technique enables simple design and relatively simple cloak structure (assuming that materials with required properties are available) and has the possibility of realization of cloaks composed of isotropic and homogeneous materials. In some cases, especially when impenetrable objects need to be cloaked, it may be problematic to find natural materials with required properties, such as very low permittivity or permeability. At some specific frequencies so-called plasmonic materials [41] can be used, but for example in the microwave regime artificial materials may be required [128]. Limitations in operation bandwidth when using artificial (often resonant) materials should be also taken into account.

In addition, there exists the fundamental limitation on the energy velocity when cloaking impenetrable objects in free space with passive structures: for the ideal operation of a cloak, the energy of an electromagnetic wave should go around the cloaked object faster than the speed of light [42] and this is of course impossible to achieve at least with passive materials and structures. This fundamental limitation will inevitably cause scattering of power, but this scattering may not be observable in frequency domain simulations which consider only time-harmonic waves. If the object to be cloaked is not impenetrable, e.g., it consists of a dielectric material, power can flow through the object and this obviously relaxes the limitations regarding bandwidth and cloaking from waves that carry energy.

5.5.2 Coordinate-transformation technique

The coordinate transformation technique, introduced by Leonhardt in [34] and Pendry *et al.* in [35], is based on the transformation of the spatial coordinates in such a way that a point in the "electromagnetic space" is transformed into a sphere (or some other shape) in the "physical space." Electromagnetic fields travelling in the physical space are forced to go around this spherical region where the coordinates are transformed, as demonstrated by Fig. 5.7. The same approach can be simplified to a two-dimensional problem, where a line is transformed into a cylinder [135]. This cloaking approach is also related to certain mathematical problems studied in the literature [136, 137].

The realization of a coordinate transformation cloak requires that inside a certain annular region in the physical space, the refractive index changes with the position in order to "squeeze" all electromagnetic fields inside the annulus, thus preventing the fields from entering the region enclosed by the annulus, i.e., the cloaked region. This type of squeezing can be realized with a refractive index that changes radially inside the annulus. In order to preserve impedance matching between the annulus (i.e., the "cloak") and the surrounding medium, the material filling the annulus must be anisotropic [35]. Although the concept of this cloaking method was introduced to a wide audience only recently, the idea of an inhomogeneous and anisotropic magneto-dielectric structure that allows a plane wave to pass through it without distortions, was published already in 1961 by Dollin [138].

In addition to the references given above, the coordinate transformation technique has been studied extensively during the past few years, resulting in a large amount of publications describing various theoretical and numerical analysis methods, practical cloak designs for different frequency regions from microwaves to optics, and experimental proof of the cloaking phenomenon [139–174]. In principle, the design of cloaks based on the coordinate transformation technique is relatively straightforward since the required material parameters are obtained directly from the transformation of coordinates. In practice the needed types of materials are difficult to realize and therefore many simplifications of the ideal coordinate transformation have been

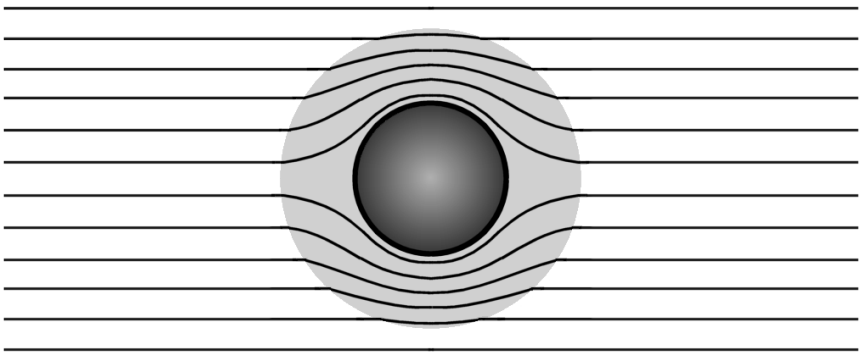

Figure 5.7: Illustration of the principle of cloaking using the coordinate transformation technique. A spherical volume in the physical space (dark grey area) is covered by an annulus (light grey area) in which electromagnetic fields are "squeezed." The black solid lines illustrate ray trajectories of electromagnetic waves that travel inside and outside the cloak.

suggested, e.g., [135, 147–149, 153]. As compared to other cloaking techniques, the benefit of the coordinate transformation technique is that the cloak design is independent of the cloaked object's shape and constitutive material (since the fields inside the cloak are zero). The most significant drawback of this technique is the difficulty of the realization of materials with suitable properties, especially when wide operation bandwidth is required. Also the fundamental problem of energy velocity exists when cloaking objects in free space. As discussed in Section 5.5.1, ideal cloaking in this case requires that the energy of the wave that "bends" around the cloaked object travels with a superluminal velocity. As opposed to the scattering cancellation technique the coordinate transformation technique is somewhat more limited by this problem of energy velocity since regardless of the object to be cloaked, the fields cannot travel through the cloaked region.

5.5.3 Other cloaking techniques

There exist also other techniques that can be regarded as at least some forms of cloaking. One is the use of so-called hard surfaces, with which the forward scattering from an object, and thus also the total scattering cross section, can be significantly reduced [175, 176]. This technique has been proposed to be used for reducing the scattering from antenna struts that normally is very harmful for an antenna's directivity pattern [175]. This technique is somewhat limited as a true cloaking technique since the total scattering cross section of an object can be lowered only concerning waves impinging on this object with a fixed angle of arrival. This is due to the

fact that with this technique, the scattering object is placed inside a cover which is elongated in the direction of expected wave propagation. For waves impinging from other angles of arrival to such a device, the total scattering cross section may actually be increased.

In papers [177–179] a way of cloaking objects situated close to a plasmonic cylinder is studied. This cloaking phenomenon is based on the excitation of surface waves at the interface between such a cylinder and, e.g., free space. In view of possible applications, this cloaking phenomenon is rather limited, since the realization of materials with suitable properties is a big challenge as such. Due to the required excitation of the surface plasmons, the cloak operation will be inevitably limited to a very narrow bandwidth and losses that are present in any realizable plasmonic material, may mitigate the cloaking phenomenon.

Very recently it was discovered that for cloaking of cylindrical objects a structure somewhat similar to the transition layer of the cloaks in [**VIII**–**X**] but composed of solid metal sheets can be used for efficient and broadband cloaking [180]. In this case the cloaked object can be a solid cylinder since within this cylindrical cloaked region there are no transmission lines. The cloaking phenomenon results from the squeezing of the fields between adjacent cone-shaped metal sheets. The fields do not penetrate the cloaked region due to the fact that the mode at the inner boundary of the annular cloak cannot couple to the narrow section of free space that is between the cloak and the cloaked object. Instead, the wave is guided around the cloaked object similar to the coordinate transformation cloaks. As there is no resonant material involved, the resulting cloaking effect is quite broadband.

5.6 Summary of related publications

Paper [**VI**] presents the principle of utilizing transmission-line networks in cloaking applications. The performance potentials of two different types of networks, namely, loaded and unloaded ones, are discussed and their benefits and drawbacks are evaluated. For the design of both types of networks, the dispersion relation is derived in a simple form. It is concluded that for practical applications that require simple structures and wide operation bandwidth, the unloaded networks offer better performance. The effect of the inevitable non-idealities of the unloaded networks, that occur when cloaking objects situated in free space, is studied and it is found that good cloaking performance can be achieved especially with electrically small cloaks. A simple way of coupling electromagnetic fields between a network of transmission lines and any homogeneous medium is proposed. The coupling phenomenon is confirmed by designing an example network and conducting numerical simulations of a slab composed of this network.

In [**VII**] a two-dimensional transmission-line network is simulated, manufactured and measured. The measurements are conducted in a parallel-plate waveguide en-

vironment to emulate an infinitely high periodic structure. The expected coupling between the network and the surrounding medium is confirmed with both measurements and numerical simulations.

Paper [**VIII**] presents a design of a cylindrical cloak based on periodically stacked two-dimensional transmission-line networks. A way of employing the previously introduced coupling method [**VI**,**VII**] in a cylindrical cloak is presented. In order to obtain a very good cloaking performance, the cloak diameter is made smaller than half of the wavelength of the impinging radiation. The cloaking effect is verified with numerical simulations. The operation of the device is confirmed also with measurements. To enable simple analysis of the frequency response of the realized cloak, the measurements are conducted with a rectangular waveguide, inside which cloaked and uncloaked objects are placed.

Paper [**IX**] gives further verification of the cloaking effect observed in [**VIII**]. Numerical simulations of field distributions of cloaked and uncloaked objects placed both in free space and inside a waveguide are presented. Measurement results of the transmission magnitude and phase are presented for two different metallic objects that are cloaked.

In [**X**] a design of an electrically large cylindrical cloak with the diameter equal to several wavelengths of the impinging radiation, is presented. The cloak is composed of periodically stacked two-dimensional transmission-line networks. The cloaking performance of this cloak is studied with numerical simulations. In addition, the same electrically small cloak as presented in [**VIII**] is studied in an antenna scenario. The effects of placing uncloaked and cloaked metallic objects close to a dipole antenna are studied with numerical simulations. It is shown that the antenna directivity pattern is strongly affected by the uncloaked object, whereas the pattern with the cloaked object resembles the situation where the antenna is alone in free space.

6 Microwave lenses composed of transmission-line networks

6.1 Introduction

Transmission-line networks that are coupled with the medium surrounding these structures can be utilized as lenses. Traditionally, lenses are composed of dielectric materials that have certain refractive index $n = \sqrt{\varepsilon_\mathrm{r}\mu_\mathrm{r}}$ different from that in the medium surrounding the lens. For example, in free space $n = 1$ and in dielectric materials usually $n > 1$ and $\varepsilon_\mathrm{r} > 1$ while $\mu_\mathrm{r} = 1$. The wave impedance in a homogeneous material is defined as

$$\eta = \sqrt{\frac{\mu}{\varepsilon}} = \sqrt{\frac{\mu_\mathrm{r}\mu_0}{\varepsilon_\mathrm{r}\varepsilon_0}}. \tag{6.1}$$

When using dielectric lenses, there is an unavoidable impedance mismatch between the medium comprising the lens and the medium surrounding the lens since the wave impedances of these media differ due to the difference in the relative permittivity ε_r. One solution to this impedance mismatch is to use magneto-dielectric materials, i.e., materials that have $\varepsilon_\mathrm{r} \neq 1$ and $\mu_\mathrm{r} \neq 1$. In free space $\varepsilon_\mathrm{r} = \mu_\mathrm{r} = 1$, and the wave impedance is approximately equal to $\eta_0 \approx 377\ \Omega$. Therefore, perfect impedance-matching with free space requires that $\varepsilon_\mathrm{r} = \mu_\mathrm{r}$. The drawback of magneto-dielectric materials is that they are not readily found in nature, and the artificial magneto-dielectric materials suffer from high losses and restricted bandwidth, since usually artificial magnetism is achieved with using resonant inclusions in the material. Another way to mitigate the impedance mismatch problem is to cover a lens with a dielectric layer of intermediate permittivity. This and other alternative solutions to the impedance mismatch problem are discussed more in Section 6.4.

Transmission-line networks can be designed to have a certain index of refraction, and at the same time, the impedance of the network can be controlled by controlling the impedance of single sections of transmission line. By coupling electromagnetic waves between such a network and a homogeneous material surrounding this network, we can realize "materials" that have engineered dispersion properties (refractive index) and that can be designed for the optimal operation depending on the application in mind.

Lenses composed of transmission-line networks can offer also other advantages with respect to homogeneous dielectric lenses or various types of artificial dielectric lenses. These benefits include weight reduction, easy implementation of electrically controllable elements such as varactors, and the use of embedded sources. Weight reduction is possible since the whole volume of a transmission-line lens is not necessarily used. If the transmission lines are placed periodically, the volume between adjacent sections of transmission line is not used for power transportation. In principle this

volume can therefore be removed from the lens which will reduce the total weight of such a lens. Of course the metal traces that compose the transmission lines add some weight, but these traces can be made very thin. The loading of transmission-line networks with controllable elements such as varactors was discussed in Chapter 4. Such loading can potentially be used to create lenses with electrically tunable index of refraction. In [**V**] this method was used to obtain a tunable negative index of refraction in a parallel-sided slab, but the same principle can of course be utilized also in lenses such as studied in this chapter.

The results presented in this chapter have been published in [**XI**,**XII**]. In addition, the author has contributed to several other papers related to this field of research [181–183].

6.2 Design principles

The design of transmission-line based microwave lenses relies on the analysis of dispersion (refractive index) and the characteristic impedance of transmission-line networks. Equations (4.1) – (4.9) can be readily used in the design of one-, two-, and three-dimensional loaded and unloaded transmission-line networks. Because here we are interested in replacing a homogeneous dielectric material with a transmission-line network, there is no need to load the network in any way. This also results in simpler design, manufacturing and broader bandwidth because of almost linear dispersion [**XI**].

Because of simplicity, here we study only two-dimensional transmission-line networks. Practically realizable lenses can be built using these, since the networks can be conveniently stacked on top of another to create volumetric structures. In the case of an unloaded two-dimensional transmission-line network, the dispersion equation (4.5) reduces to

$$\cos(k_x d) + \cos(k_y d) = 4\cos^2(k_{\mathrm{TL}} d/2) - 2, \tag{6.2}$$

and the characteristic impedance of the network is described by (4.9).

Equation (6.2) can be used to analyze the isotropy of the network, but at the frequencies where the network exhibits isotropic or nearly isotropic propagation characteristics, the refractive index of waves travelling in this network is simply [**XI**]

$$n = \sqrt{2\varepsilon_{\mathrm{eff,TL}}}\,, \tag{6.3}$$

where $\varepsilon_{\mathrm{eff,TL}}$ is the effective relative permittivity of the transmission lines composing the network. For the optimal performance, the characteristic impedance of the network should be designed to match the wave impedance in the material surrounding this network. As can be concluded from (4.9) and from the results presented in [**VI**,**XI**], the matching of the network impedance usually requires very large values of Z_{TL} (several hundreds of Ohms). Such high values may not be achievable with conventional transmission lines, e.g., parallel strips or microstrips.

For the transmission-line topologies used in this thesis the use of a transition layer, such as described in Chapters 4 and 5, is required to couple the electromagnetic waves between the lens and the surrounding medium. The use of such layers also relaxes the demands on the characteristic impedance: the transition layer can effectively couple the waves between a transmission-line network and a homogeneous medium, such as free space, even though the characteristic impedance of the network does not match the wave impedance in the surrounding medium [**V**].

6.3 Analytical and numerical results

A volumetric lens composed of periodically stacked two-dimensional transmission-line networks is proposed and designed in [**XI**]. The surface profile of the lens is designed with the well known equations for dielectric lens design [184] so that a plane wave impinging on the lens is focused into a line on the other side of the lens. With the dispersion equation (6.2) describing the wave propagation in the used type of network, it is easy to calculate the effective refractive index in the network and design the lens profile as in the case of a homogeneous dielectric lens having the same refractive index. In the network design it should be taken into account that the period of the network must be small enough as compared to the wavelength, so that propagation inside the network is effectively isotropic. Otherwise the refraction at the lens interface will not be as desired.

In the structure studied here, the parallel-strip transmission lines are completely embedded in a dielectric with permittivity $\varepsilon_\mathrm{r} = 2.33$, and therefore $\varepsilon_\mathrm{eff,TL} = \varepsilon_\mathrm{r} = 2.33$ in this case. The resulting refractive index of the network is thus $n = \sqrt{4.66} \approx 2.16$, according to (6.3). The dispersion in the network is plotted for the axial propagation in Fig. 6.1a, where also the free space propagation constant ("light line") and the dispersion curve in a homogeneous dielectric with $n = \sqrt{4.66}$ are shown. The period of the network defines the upper frequency limit where the wave propagation is effectively isotropic. Here the period of the network d is equal to 8 mm and the network is effectively isotropic up to approximately 3 GHz, but the difference in the wavenumbers of diagonal and axial propagation is very small even at 4 GHz, as can be concluded from Fig. 6.1a (the diagonal propagation follows the same curve as that of the homogeneous dielectric).

The lens surface profile is illustrated in Fig. 6.1b, where also the structure of the network and the transition layer are illustrated. The profile is calculated with [184]

$$y^2 = (n^2 - 1)(x - F)^2 + 2(n - 1)F(x - F), \tag{6.4}$$

where x is the distance from the focal point in the direction parallel to the lens axis and F is the focal distance. For the lens studied here $F = 80d$. The reader should note that in (6.4) the origin of the coordinate system is at the focal point, whereas in Fig. 6.1b the origin is at the corner of the lens.

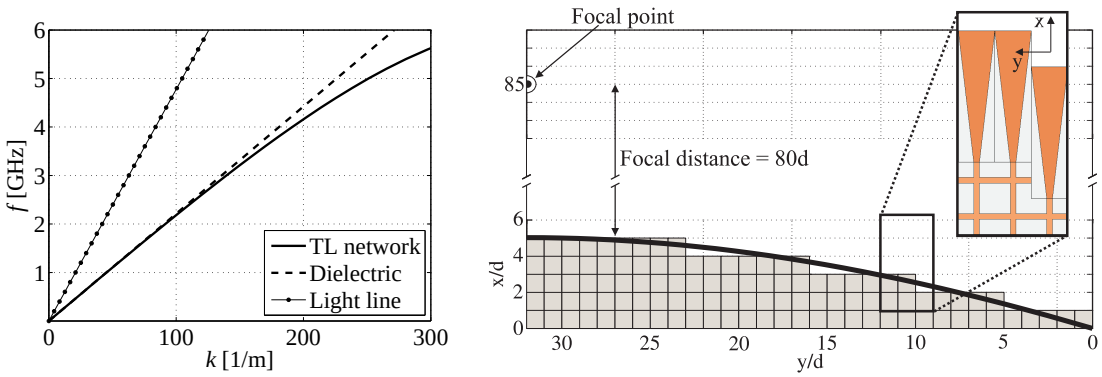

(a) (b)

Figure 6.1: From [**XI**]. (a) Dispersion in a transmission-line (TL) network for axial propagation ($k_y = 0$, $k = k_x$), in a homogeneous dielectric material with $\varepsilon_\mathrm{r} = 4.66$ and in free space ("light line"). (b) Analytically calculated lens surface profile (thick black line) and the transmission-line network (each square represents one unit cell of the network) having approximately the same profile. Only half of the lens is shown along the y-axis since the simulation model is cut in half by a PMC boundary, positioned at $y = 32d$. The inset illustrates the details of the simulated transmission-line lens structure.

As the lens is composed of periodic unit cells, it is impossible to realize a lens with a smooth surface profile. On the other hand, the unit cell size is so small as compared to the wavelength that the lens refraction characteristics are basically the same as those of a lens with a smooth profile. The lens operation is demonstrated in [**XI**] by comparing the designed transmission-line lens to a dielectric lens having the same surface profile. The operation of the lenses is studied by comparing the field distributions in the free space that surrounds them. This analysis is conducted with full-wave simulations of the lenses. Two scenarios are studied: 1) A plane wave travelling in the direction of the positive x-axis and having the electric field parallel to the z-axis (see Fig. 6.1b for the geometry) and 2) A line source placed at the focal point of the lenses.

In the first case the refraction occurring at the interfaces of the lenses is studied and compared, which leads to the conclusion that the lenses refract the impinging waves similarly, focusing an impinging plane wave to a line. The reduction of unwanted reflections from the transmission-line lens, as compared to the dielectric lens, is also observed. The reflectances of the two lenses are computed as functions of the frequency, demonstrating that the relative bandwidth where the reflectance of the transmission-line lens is lower than that of the dielectric lens by 4 dB or more, is wider than 16 percent [**XI**]. The lowest reflectance of the transmission-line lens, approximately -18 dB, is observed at the frequency of 2.4 GHz. At this frequency the reflectance of the dielectric lens is approximately -6 dB.

In the second case a line source, positioned at the focal point, illuminates the transmission-line lens and the dielectric lens. Also here the lenses are seen to operate as expected, i.e., a plane wave field travelling in the direction of the negative x-axis is created. The simulated field distributions indicate that, as compared to the dielectric lens, the reflections from the transmission-line lens are clearly mitigated [**XI**].

A microwave lens composed of the same transmission-line network as that described above, but with an embedded source, is studied in [**XII**]. The embedding is enabled by choosing such a lens profile where the surface nearest to the focal point of the lens is cylindrical. Again we essentially study a two-dimensional problem since the lens is considered to be infinitely periodic in the vertical direction. Such a lens profile can be designed with equations available in, e.g., [184]. In this case the inner lens surface, i.e., the surface closer to the focal point, is cylindrical with distance F from the focal point. The other surface of the lens is defined as [184]

$$y^2 = \frac{[x + (n-1)(F+T)]^2}{n^2} - x^2, \tag{6.5}$$

where x is the distance from the focal point in the direction parallel to the lens axis, F is the focal distance, and T is the thickness of the lens. See Fig. 6.2a for the lens profile in the case $n = \sqrt{4.66}$. The reason why we have chosen to use this geometry is that the volume between the focal point and the lens can be filled with any homogeneous isotropic material, without affecting refraction at the lens surfaces. This enables the embedding of a source into a transmission-line lens having this geometry, since the volume between the source (placed at the focal point) and the lens surface can be filled with the same transmission-line network as composes the lens itself. Such a lens is illustrated in Fig. 6.2b.

In [**XII**] this lens antenna is studied with numerical simulations and its directivity is compared to two dielectric lens antennas having the same surface profile and refractive index. One dielectric antenna has a step-wise surface profile similar to the transmission-line lens antenna while the other has a smooth surface profile. The results indicate that the directivity of the transmission-line lens antenna is much higher than the dielectric antennas'. This is concluded to be a result of the reduced reflections at the interfaces between the lenses and the surrounding free space, as well as a result of the fact that the sidelobe level of the transmission-line lens antenna is reduced dramatically by introducing lumped resistors at the side edges of this lens. This of course lowers the radiation efficiency of this antenna which makes the comparison between the studied antennas rather difficult since the dielectric antennas are modelled as lossless. Nevertheless, [**XII**] gives further confirmation of the fact that transmission-line lenses can be effectively homogenized and designed using well-known analytical expressions derived for dielectric lenses. The good coupling of electromagnetic fields between such lenses and free space is also evident.

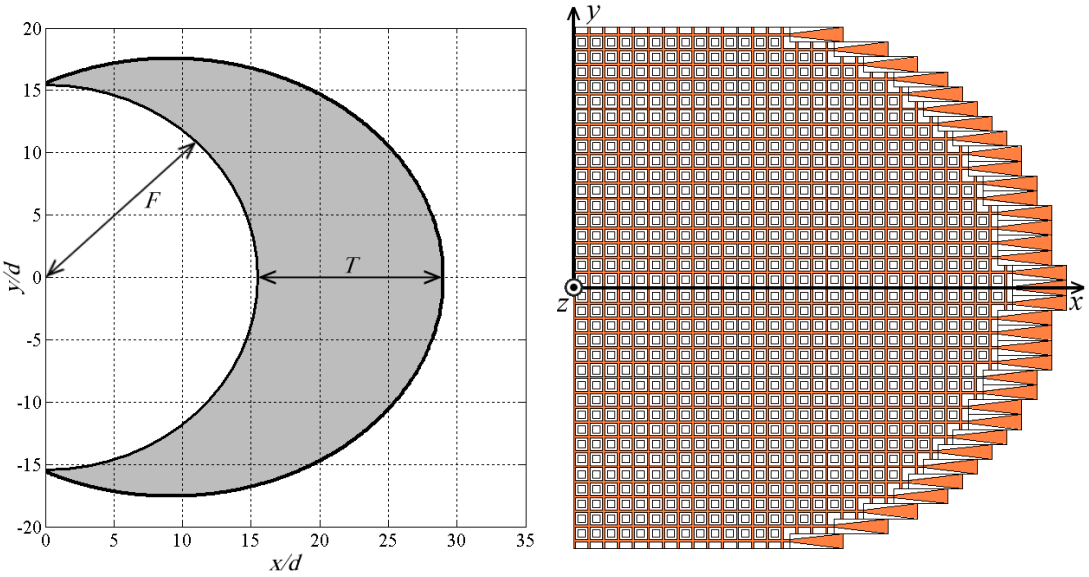

(a) (b)

Figure 6.2: From [**XII**]. (a) Lens profile, calculated with (6.5), having $F = 15.5d$, $T = 13.5d$, $d = 8$ mm, and $n = \sqrt{4.66}$. The source location is at $x = 0$, $y = 0$. (b) Model of the proposed transmission-line lens antenna with the same surface profile as the lens in (a). The period d of the network is equal to 8 mm, and the size of the antenna in the transversal (y-) direction is $35d = 280$ mm.

6.4 Review of related results found in the literature

Dielectric lenses have been widely studied and used for decades. There exists a variety of literature related to dielectric lens design, including also many ways of reducing the effects of impedance mismatch inherent to such lenses [184–188]. Here we review some basic techniques that can be used to reduce reflections at lens interfaces and also some lens design techniques that employ transmission lines.

6.4.1 Ways to mitigate the impedance mismatch problem in dielectric lenses

The mismatch between the wave impedances of two dielectric materials is simply due to the difference in the relative permittivity ε_r. From (6.1) we see that the ratio between the wave impedances in free space (η_0) and in a dielectric material (η) is proportional to the square root of the relative permittivity of the dielectric:

$$\frac{\eta_0}{\eta} = \frac{\sqrt{\frac{\mu_0}{\varepsilon_0}}}{\sqrt{\frac{\mu_0}{\varepsilon_\mathrm{r}\varepsilon_0}}} = \sqrt{\varepsilon_\mathrm{r}}. \tag{6.6}$$

As ε_r increases, the refractive index $n = \sqrt{\varepsilon_\mathrm{r}}$ increases and the impedance mismatch also grows larger. One obvious way to mitigate the reflections from dielectric lenses is therefore to restrict the permittivity of the lens material to values close to $\varepsilon_\mathrm{r} = 1$. This results in problems with the size of the lens as the refraction angle at the lens surface is almost equal to the incidence angle.

If a dielectric material with large permittivity is required because of practical design issues, the lens can be effectively coupled with free space by using a quarter-wave layer of intermediate permittivity material [184, 186]. The drawbacks of this technique are the increase of the lens thickness, more complicated manufacturing, and the frequency dependence of the matching. The layer of intermediate permittivity can be also realized by cutting grooves on the surface of the dielectric lens itself, which lowers the effective permittivity in the area where the grooves are situated. Practical engineering problems however limit the use of these techniques at high frequencies. In [184] it is reported that these techniques are difficult to realize for lenses operating at or above the K_u-band (12 GHz – 18 GHz). The reason is that as the wavelength gets smaller, the manufacturing errors, etc. will result in gain drop and sidelobe level degradation.

6.4.2 Artificial dielectric lenses

Artificial dielectrics have been used for a long time in lenses [8, 9]. Artificial dielectrics can be designed to have refractive index n larger or smaller than unity, see, e.g., [43, 48, 189]. Materials with $n < 1$ can be used in lenses that are impossible to create with "natural" dielectrics which always have $n > 1$. But artificial dielectrics with $n > 1$ have also been found to be useful in many applications. For example, weight reduction of lenses with the use of artificial dielectrics has been recently studied [48]. Artificial dielectrics, whether they have the refractive index larger or smaller than unity, have the same impedance mismatch problem as any dielectric material.

6.4.3 Constrained lenses

A constrained lens consists of radiating elements, such as antennas, situated at the lens surfaces and of transmission lines that connect the elements at these surfaces [184, 190]. The lens effect is achieved by using transmission lines of different lengths. Usually the transmission lines in these types of lenses are one-dimensional, i.e., a receiving antenna at the first lens surface is connected by a transmission line to another antenna at the other lens surface. These lenses can be designed to have similar lens properties as dielectric lenses, but only in a certain frequency band, since the optimal electrical lengths of the transmission lines are designed for a specific frequency.

6.5 Summary of related publications

Paper [**XI**] presents the principle of utilizing transmission-line networks as artificial materials for lenses. An example lens that focuses a plane wave to a line, is designed based on analytical expressions for dispersion and lens surface profile. The lens operation is verified with numerical simulations and the results are compared to those of a reference dielectric lens. It is shown that within a certain frequency band the reflections at the surface of the transmission-line lens are mitigated as compared to the reference case.

A microwave lens antenna based on a volumetric transmission-line structure is presented and studied in [**XII**]. The network design is the same as in [**XI**], but the lens profile is different to enable embedding of a source in the transmission-line network. The operation of this lens antenna is verified with numerical simulations. The directivity pattern of the lens antenna is evaluated with numerical simulations and the results are compared to directivity patterns of two lens antennas composed of a homogeneous dielectric material, demonstrating the improvement of the directivity in the case of the transmission-line lens antenna.

7 Conclusions

This thesis consists of a collection of results related to the applications of microwave transmission-line networks in three specific areas of interest: backward-wave media, electromagnetic cloaking, and lenses. These topics have attracted a constantly increasing interest in the scientific community during the last years. Metamaterials that are usually employed in the creation of backward-wave media and cloaking devices can be realized in many ways. The use of transmission-line networks and especially such networks that can be used for free-space excitation, have many benefits as compared to other realizable metamaterials. These benefits include the possibility to obtain wide bandwidths and non-resonant media, as well as the ease of manufacturing and assembly.

Backward-wave media are interesting due to their potential use in imaging systems. A special characteristic of such media is that they enable imaging with resolution exceeding the diffraction limit. This type of imaging is usually referred to as subwavelength imaging. In this thesis backward-wave media, realized with capacitively and inductively loaded three-dimensional transmission-line networks, are studied analytically, numerically, and experimentally. Backward-wave propagation in the proposed type of circuit topology is confirmed both with numerical simulations and measurements. A way of coupling a transmission-line network with a homogeneous medium, such as free space, is presented. A slab composed of a three-dimensional transmission-line network exhibiting backward-wave propagation in a certain frequency range, is coupled with free space using the proposed method and the efficiency of this coupling is confirmed with numerical simulations. Furthermore, the electrical tunability of the refractive index of such a slab is studied both analytically and numerically.

Electromagnetic cloaking means – in the context of this thesis – the reduction of an object's total scattering cross section. A novel method of achieving efficient and broadband cloaking of a class of objects having a limited size and shape, is proposed. This method employs volumetric structures composed of transmission-line networks. By coupling these network with the surrounding medium (e.g., free space) the electromagnetic wave which impinges on the cloaking device, and on the cloaked object enclosed by this device, is tunnelled through the cloaked object inside the transmission lines. Within this thesis, the basic principles, possibilities, and limitations of this cloaking method are discussed. An example cloak, operating in the microwave region, is designed and its performance is evaluated numerically and experimentally. The main advantages offered by the proposed cloaking method, namely, wide operation bandwidth and ease of manufacturing and assembly, are confirmed with both numerical simulations and measurements.

Dielectric lenses are widely used as collimating elements in antennas. The inherent impedance mismatch between such a lens and the medium surrounding this lens causes reflections at the lens surfaces and thus loss of power, radiation in unwanted

directions, and deterioration of the directivity of the antenna. There exist many ways of reducing these unwanted reflections, but they all have some limitations and drawbacks. In this thesis we propose a way of realizing microwave lenses by using volumetric transmission-line networks as the media composing the lenses. This enables the engineering of the dispersion and impedance properties of such lenses with possibility to improve the impedance characteristics for better matching. Two example lenses are designed and their performance is evaluated with numerical simulations.

As the basic concepts and design principles of various structures based on transmission-line networks have been well established in the recent literature and in the context of this thesis, the future research of such structures can be aimed on the design and optimization of various practical devices. Applications that can potentially benefit from the advantages offered by such structures include, for example, antennas, imaging, high-resolution sensing, and reduction of scattering. As transmission-line networks are studied and developed further, completely new ideas of applications and devices may also appear. Especially the potential in creating transmission-line based structures with electrically tunable properties, such as the refractive index, may be a significant benefit of these structures in view of future applications.

References

[1] S. Tretyakov, *Analytical modeling in applied electromagnetics*, Norwood, MA: Artech House, 2003.

[2] G. V. Eleftheriades and K. G. Balmain, Eds., *Negative-refraction metamaterials: fundamental principles and applications*, Hoboken, NJ: John Wiley & Sons, 2005.

[3] C. Caloz and T. Itoh, *Electromagnetic metamaterials: Transmission line theory and microwave applications*, Hoboken, NJ: John Wiley & Sons, 2006.

[4] M. Lapine and S. Tretyakov, "Contemporary notes on metamaterials," *IET Microw. Antennas Propag.*, vol. 1, no. 1, pp. 3–11, 2007.

[5] A. Sihvola, "Metamaterials in electromagnetics," *Metamaterials*, vol. 1, no. 1, pp. 2–11, 2007.

[6] E. Shamonina and L. Solymar, "Metamaterials: How the subject started," *Metamaterials*, vol. 1, no. 1, pp. 12–18, 2007.

[7] C. R. Simovski and S. A. Tretyakov, "Local constitutive parameters of metamaterials from an effective-medium perspective," *Phys. Rev. B*, vol. 75, no. 19, p. 195111, 2007.

[8] W. E. Kock, "Metal-lens antennas," *Proc. IRE*, vol. 34, pp. 828–836, 1946.

[9] W. E. Kock, "Metallic delay lenses," *Bell System Tech. J.*, vol. 27, pp. 58–82, 1948.

[10] N. Engheta and R. W. Ziolkowski, Eds., *Electromagnetic metamaterials: Physics and engineering explorations*, Wiley-IEEE Press, 2006.

[11] V. M. Shalaev and A. K. Sarychev, *Electrodynamics of metamaterials*, World Scientific Publishing Company, 2007.

[12] C. M. Krowne and Y. Zhang, Eds., *Physics of negative refraction and negative index materials: Optical and electronic aspects and diversified approaches*, Springer Series in Materials Science, Springer, 2007.

[13] R. Marques, F. Martin, and M. Sorolla, *Metamaterials with negative parameters: Theory, design and microwave applications*, Wiley Series in Microwave and Optical Engineering, Wiley-Interscience, 2008.

[14] P. Markos and C. M. Soukoulis, *Wave propagation: From electrons to photonic crystals and left-handed materials*, Princeton University Press, 2008.

[15] S. A. Ramakrishna and T. M. Grzegorczyk, *Physics and applications of negative refractive index materials*, New York: CRC Press, 2009.

[16] L. Solymar and E. Shamonina, *Waves in metamaterials*, Oxford University Press, 2009.

[17] F. Capolino, Ed., *Handbook of artificial materials*, New York: CRC Press, 2009.

[18] V. G. Veselago, "The electrodynamics of substances with simultaneously negative values of ε and μ" *Soviet Physics Uspekhi*, vol. 10, no. 4, pp. 509–514, 1968 (originally published in Russian in 1967).

[19] D. R. Smith, W. J. Padilla, D. C. Vier, S. C. Nemat-Nasser, and S. Schultz, "Composite medium with simultaneously negative permeability and permittivity," *Phys. Rev. Lett.*, vol. 84, no. 18, pp. 4184–4187, 2000.

[20] R. A. Shelby, D. R. Smith, and S. Schultz, "Experimental verification of a negative index of refraction," *Science*, vol. 292, no. 5514, pp. 77–79, 2001.

[21] J. B. Pendry, *Phys. Rev. Lett.*, vol. 85, no. 18, pp. 3966–3969, 2000.

[22] I. V. Lindell, S. A. Tretyakov, K. I. Nikoskinen, and S. Ilvonen, "BW media – Media with negative parameters, capable of supporting backward waves," *Microwave Opt. Technol. Lett.*, vol. 31, no. 2, pp. 129–133, 2001.

[23] D. R. Smith and N. Kroll, "Negative refractive index in left-handed materials," *Phys. Rev. Lett.*, vol. 85, no. 14, pp. 2933–2936, 2000.

[24] D. R. Smith, J. B. Pendry, and M. C. K. Wiltshire, "Metamaterials and negative refractive index," *Science*, vol. 305, no. 5685, pp. 788–792, 2004.

[25] A. Sihvola, *Electromagnetic mixing formulas and applications*. London: IEE Electromagnetic Wave Series, 1999.

[26] S. A. Schelkunoff and H. T. Friis, *Antennas: Theory and practice*. New York: John Wiley & Sons, 1952.

[27] W. N. Hardy and L. A. Whitehead, "Split-ring resonator for use in magnetic resonance from 200–2000 MHz," *Rev. Sci. Instrum.*, vol. 52, no. 2, pp. 213–216, 1981.

[28] I. V. Lindell, A. H. Sihvola, S. A. Tretyakov, and A. J. Viitanen, *Electromagnetic waves in chiral and bi-isotropic media*. Norwood, MA: Artech House, 1994.

[29] A. Serdyukov, I. Semchenko, S. Tretyakov, and A. Sihvola, *Electromagnetics of bi-anisotropic materials: Theory and applications*. Amsterdam: Gordon and Breach Science Publishers, 2001.

[30] C. G. Parazzoli, R. B. Greegor, K. Li, B. E. C. Koltenbah, and M. Tanielian, "Experimental verification and simulation of negative index of refraction using Snell's law," *Phys. Rev. Lett.*, vol. 90, no. 10, p. 107401, 2003.

[31] A. A. Houck, J. B. Brock, and I. L. Chuang, "Experimental observations of a left-handed material that obeys Snell's law," *Phys. Rev. Lett.*, vol. 90, no. 13, p. 137401, 2003.

[32] M. Born and E. Wolf, *Principles of optics*, 6th ed., Cambridge: University Press, 1998.

[33] A. Alù and N. Engheta, "Achieving transparency with plasmonic and metamaterial coatings," *Phys. Rev. E*, vol. 72, no. 1, p. 016623, 2005.

[34] U. Leonhardt, "Optical conformal mapping," *Science*, vol. 312, no. 5781, pp. 1777–1780, 2006.

[35] J. B. Pendry, D. Schurig, and D. R. Smith, "Controlling electromagnetic fields," *Science*, vol. 312, no. 5781, pp. 1780–1782, 2006.

[36] P. Ufimtsev, "New insight into the classical Macdonald physical optics approximation," *IEEE Antennas Propag. Magazine*, vol. 50, no. 3, pp. 11–20, 2008.

[37] M. Kerker, "Invisible bodies," *J. Opt. Soc. Am.*, vol. 65, no. 4, pp. 376–379, 1975.

[38] H. Chew and M. Kerker, "Abnormally low electromagnetic scattering cross sections," *J. Opt. Soc. Am.*, vol. 66, no. 5, pp. 445–449, 1976.

[39] N. G. Alexopoulos and N. K. Uzunoglu, "Electromagnetic scattering from active objects: invisible scatterers," *Applied Optics*, vol. 17, no. 2, pp. 235–239, 1978.

[40] A. Sihvola, "Properties of dielectric mixtures with layered spherical inclusions," in *Microwave radiometry and remote sensing applications*, P. Pampaloni, Ed., Utrecht, the Netherlands: VSP, 1989, pp. 115–123.

[41] A. Alù and N. Engheta, "Plasmonic and metamaterial cloaking: Physical mechanisms and potentials," *J. Opt. A*, vol. 10, p. 093002, 2008.

[42] P. Alitalo and S. Tretyakov, "Electromagnetic cloaking with metamaterials," *Materials Today*, vol. 12, no. 3, pp. 22–29, 2009.

[43] J. B. Brown, "Artificial dielectrics having refractive indices less than unity," *Proc. IEE*, vol. 100, no. 4, pp. 51–62, 1953.

[44] R. C. Hansen and M. Burke, "Antenna with magneto-dielectrics," *Microwave Opt. Technol. Lett.*, vol. 26, no. 2, pp. 75–78, 2000.

[45] H. Mosallaei and K. Sarabandi, "Magneto-dielectrics in electromagnetics: Concept and applications," *IEEE Trans. Antennas Propag.*, vol. 52, no. 6, pp. 1558–1567, 2004.

[46] S. A. Tretyakov, S. I. Maslovski, A. A. Sochava, and C. R. Simovski, "The influence of complex material coverings on the quality factor of simple radiating systems," *IEEE Trans. Antennas Propag.*, vol. 53, no. 3, pp. 965–970, 2005.

[47] P. M. T. Ikonen, K. N. Rozanov, A. V. Osipov, P. Alitalo, and S. A. Tretyakov, "Magnetodielectric substrates in antenna miniaturization: Potential and limitations," *IEEE Trans. Antennas Propag.*, vol. 54, no. 11, pp. 3391–3399, 2006.

[48] P. Ikonen, *Artificial electromagnetic composite structures in selected microwave applications*, Helsinki University of Technology: PhD Dissertation, 2007.

[49] D. M. Pozar, *Microwave engineering*, 3rd ed., Hoboken, NJ: John Wiley & Sons, 2005.

[50] R. E. Collin, *Field theory of guided waves*, 2nd ed., Piscataway, NJ: IEEE Press, and Oxford, England: Oxford University Press, 1991.

[51] A. K. Iyer and G. V. Eleftheriades, "Negative refractive index metamaterials supporting 2-D waves," *Proc. IEEE MTT-S International Microwave Symposium*, Seattle, USA, June 2–7, 2002, vol. 2, pp. 1067–1070.

[52] C. Caloz, H. Okabe, T. Iwai, and T. Itoh, "Transmission line approach of left-handed (LH) materials," *Proc. USNC/URSI National Radio Science Meeting*, San Antonio, USA, June 16–21, 2002, vol. 1, p. 39.

[53] C. Caloz and T. Itoh, "Application of the transmission line theory of left-handed (LH) materials to the realization of a microstrip LH line," *Proc. IEEE Antennas and Propagation Society International Symposium*, San Antonio, USA, June 16–21, 2002, vol. 2, pp. 412–415.

[54] A. A. Oliner, "A periodic-structure negative-refractive-index medium with resonant elements," *Proc. USNC/URSI National Radio Science Meeting*, San Antonio, USA, June 16–21, 2002, vol. 1, p. 41.

[55] G. V. Eleftheriades, A. K. Iyer, and P. C. Kremer, "Planar negative refractive index media using periodically L-C loaded transmission lines," *IEEE Trans. Antennas Propag.*, vol. 50, no. 12, pp. 2702–2712, 2002.

[56] L. Liu, C. Caloz, C. C. Chang, and T. Itoh, "Forward coupling phenomena between artificial left-handed transmission lines," *J. Appl. Phys.*, vol. 92, no. 9, pp. 5560–5565, 2002.

[57] C. Caloz and T. Itoh, "Transmission-line approach of left-handed (LH) materials and microstrip implementation of an artificial LH transmission line," *IEEE Trans. Antennas Propag.*, vol. 52, no. 5, pp. 1159–1166, 2004.

[58] A. Grbic and G. V. Eleftheriades, "Overcoming the diffraction limit with a planar left-handed transmission-line lens," *Phys. Rev. Lett.*, vol. 92, no. 11, p. 117403, 2004.

[59] A. Grbic and G. V. Eleftheriades, "Periodic analysis of a 2-D negative refractive index transmission line structure," *IEEE Trans. Antennas Propag.*, vol. 51, no. 10, pp. 2604–2611, 2003.

[60] A. Grbic and G. V. Eleftheriades, "Negative refraction, growing evanescent waves and sub-diffraction imaging in loaded transmission-line metamaterials," *IEEE Trans. Microw. Theory Tech.*, vol. 51, no. 12, pp. 2297–2305, 2003.

[61] A. Sanada, C. Caloz, and T. Itoh, "Characteristics of composite right/left-handed transmission lines," *IEEE Microw. Wireless Compon. Lett.*, vol. 14, no. 2, pp. 68-70, 2004.

[62] A. Sanada, C. Caloz, and T. Itoh, "Planar distributed structures with negative refractive index," *IEEE Trans. Microw. Theory Tech.*, vol. 52, no. 4, pp. 1252–1263, 2004.

[63] Y. C. Chen, C. K. C. Tzuang, T. Itoh, and T. K. Sarkar, "Modal characteristics of planar transmission lines with periodical perturbations: Their behaviors in bound, stopband, and radiation regions," *IEEE Trans. Antennas Propag.*, vol. 53, no. 1, pp. 47–58, 2005.

[64] A. Grbic and G. V. Eleftheriades, "Practical limitations of subwavelength resolution using negative-refractive-index transmission-line lenses," *IEEE Trans. Antennas Propag.* vol. 53, no. 10, pp. 3201–3209, 2005.

[65] C. Caloz, "Dual composite right/left-handed (D-CRLH) transmission line metamaterial," *IEEE Microw. Wireless Compon. Lett.*, vol. 16, no. 11, pp. 585–587, 2006.

[66] J. Perruisseau-Carrier and A. Skrivervik, "Bloch wave approach to the design of optimally matched non-effective medium composite right/left handed transmission lines," *IET Microw. Antennas Propag.*, vol. 1, no. 1, pp. 50–55, 2007.

[67] G. V. Eleftheriades, "Analysis of bandwidth and loss in negative-refractive-index transmission-line (NRI-TL) media using coupled resonators," *IEEE Microw. Wireless Compon. Lett.*, vol. 17, no. 6, pp. 412–414, 2007.

[68] G. V. Eleftheriades and K. G. Balmain, Eds., *Negative-refraction metamaterials: fundamental principles and applications*, Hoboken, NJ: John Wiley & Sons, 2005, Chapter 2.

[69] I.-H. Lin, M. DeVincentis, C. Caloz, and T. Itoh, "Arbitrary dual-band components using composite rigth/left-handed transmission lines," *IEEE Trans. Microw. Theory Tech.*, vol. 52, no. 4, pp. 1142–1149, 2004.

[70] G. V. Eleftheriades and M. Antoniades, "Antenna applications of negative-refractive-index transmission-line structures," *IET Microw. Antennas Propag.*, vol. 1, no. 1, pp. 12–22, 2007.

[71] G. V. Eleftheriades and R. Islam, "Miniaturized microwave components and antennas using negative-refractive-index transmission-line (NRI-TL) metamaterials," *Metamaterials*, vol. 1, no. 2, pp. 53–61, 2007.

[72] G. V. Eleftheriades, "Enabling RF/microwave devices using negative-refractive-index transmission-line (NRI-TL) metamaterials," *IEEE Antennas Propag. Magazine*, vol. 49, no. 2, pp. 34–51, 2007.

[73] C. Caloz, T. Itoh, and A. Rennings, "CRLH metamaterial leaky-wave and resonant antennas," *IEEE Antennas Propag. Magazine*, vol. 50, no. 5, pp. 25–39, 2008.

[74] M. A. Antoniades and G. V. Eleftheriades, "A broadband series power divider using zero-degree metamaterial phase-shifting lines," *IEEE Microw. Wireless Compon. Lett.*, vol. 15, no. 11, pp. 808–810, 2005.

[75] A. C. Papanastasiou, G. E. Georghiou, and G. V. Eleftheriades, "A quad-band Wilkinson power divider using generalized NRI transmission lines," *IEEE Microw. Wireless Compon. Lett.*, vol. 18, no. 8, pp. 521–523, 2008.

[76] H. V. Nguyen and C. Caloz, "Generalized coupled-mode approach of metamaterial coupled-line couplers: Complete theory, explanation of phenomena and experimental demonstration," *IEEE Trans. Microw. Theory Tech.*, vol. 55, no. 5, pp. 1029–1039, 2007.

[77] Y. Wang, Y. Zhang, F. Liu, L. He, H. Li, H. Chen, and C. Caloz, "Simplified description of asymmetric right-handed composite right/left-handed coupler in microstrip chip technology," *Microwave Opt. Technol. Lett.*, vol. 49, no. 9, pp. 2063–2068, 2007.

[78] D. Kholodnyak, E. Serebryakova, I. Vendik, and O. Vendik, "Broadband digital phase shifter based on switchable right- and left-handed transmission line sections," *IEEE Microw. Wireless Compon. Lett.*, vol. 16, no. 15, pp. 258–260, 2006.

[79] S. Abielmona, S. Gupta, and C. Caloz, "Experimental demonstration and characterization of a tunable CRLH delay line system for impulse/continuous wave," *IEEE Microw. Wireless Compon. Lett.*, vol. 17, no. 12, pp. 864–866, 2007.

[80] H. V. Nguyen and C. Caloz, "Composite right/left-handed delay line pulse position modulation transmitter," *IEEE Microw. Wireless Compon. Lett.*, vol. 18, no. 5, pp. 527–529, 2008.

[81] P. P. Wang, M. A. Antoniades and G. V. Eleftheriades, "An investigation of printed Franklin antennas at X-band using artificial (Metamaterial) phase-shifting lines," *IEEE Trans. Antennas Propag.*, vol. 56, no. 10, pp. 3118–3128, 2008.

[82] F. Qureshi, M. A. Antoniades, and G. V. Eleftheriades, "A compact and low-profile metamaterial ring antenna with vertical polarization," *IEEE Antennas Wireless Propag. Lett.*, vol. 4, pp. 333–336, 2005.

[83] A. Lai, K. M. K. H. Leong, and T. Itoh, "Infinite wavelength resonant antennas with monopolar radiation pattern based on periodic structures," *IEEE Trans. Antennas Propag.* vol. 55, no. 3, pp. 868–876, 2007.

[84] J.-H. Park, Y.-H. Ryu, J.-G. Lee, and J.-H. Lee, "Epsilon negative zeroth-order resonator antenna," *IEEE Trans. Antennas Propag.* vol. 55, no. 12, pp. 3710–3712, 2007.

[85] F. P. Casares-Miranda, C. Camacho-Penalosa, and C. Caloz, "High-gain active composite right/left-handed leaky-wave antenna," *IEEE Trans. Antennas Propag.*, vol. 54, no. 8, pp. 2292–2300, 2006.

[86] C. Allen, K. Leong, and T. Itoh, "Design of a balanced 2D composite right-/left-handed transmission line type continuous scanning leaky-wave antenna," *IET Microw. Antennas Propag.*, vol. 1, no. 3, pp. 746–750, 2007.

[87] M. A. Antoniades and G. V. Eleftheriades, "A CPS leaky-wave antenna with reduced beam squinting using NRI-TL metamaterials," *IEEE Trans. Antennas Propag.*, vol. 56, no. 3 pp. 708–721, 2008.

[88] A. Karilainen, *Thin-sheet antennas based on networks of loaded transmission lines*, Helsinki University of Technology: Master's Thesis, 2008.

[89] P. Alitalo, *Design of a three-dimensional superlens using loaded transmission lines*, Helsinki University of Technology: Master's Thesis, 2006.

[90] S. Maslovski, S. A. Tretyakov, and P. Alitalo, "Near-field enhancement and imaging in double planar polariton-resonant structures," *J. Appl. Phys.*, vol. 96, no. 3, pp. 1293–1300, 2004.

[91] P. Alitalo, S. Maslovski, and S. Tretyakov, "Near-field enhancement and imaging in double cylindrical polariton-resonant structures: Enlarging superlens," *Phys. Lett. A*, vol. 357, no. 4–5, pp. 397–400, 2006.

[92] P. Alitalo, C. Simovski, A. Viitanen, and S. Tretyakov, "Near-field enhancement and subwavelength imaging in the optical region using a pair of two-dimensional arrays of metal nanospheres," *Phys. Rev. B*, vol. 74, no. 23, p. 235425, 2006.

[93] P. Alitalo, S. Maslovski, and S. Tretyakov, "Three-dimensional isotropic TL-based superlens," *Proc. 3rd workshop on metamaterials and special materials for electromagnetic applications and TLC*, Rome, Italy, March 30–31, 2006, p. 32.

[94] P. Alitalo, S. Maslovski, and S. Tretyakov, "Three-dimensional isotropic transmission-line superlens," *Proc. URSI EMTS 2007*, Ottawa, Canada, July 27–28, 2007, p. EMTS32.

[95] P. Alitalo, C. R. Simovsky, L. Jylhä, A. J. Viitanen, and S. A. Tretyakov, "Subwavelength imaging in the visible using a pair of arrays of metal nanoparticles," *Proc. Metamaterials'2007*, Rome, Italy, October 22–24, 2007, pp. 12–15.

[96] S. Maslovski, P. Alitalo, and S. Tretyakov, "Subwavelength imaging based on frequency scanning," *J. Appl. Phys.*, vol. 104, no. 10, p. 103109, 2008.

[97] A. Grbic and G. V. Eleftheriades, "An isotropic three-dimensional negative-refractive-index transmission-line metamaterial," *J. Appl. Phys.*, vol. 98, no. 4, p. 043106, 2005.

[98] A. K. Iyer and G. V. Eleftheriades, "A three-dimensional isotropic transmission-line metamaterial topology for free-space excitation," *Appl. Phys. Lett.*, vol. 92, no. 26, p. 261106, 2008.

[99] W. J. R. Hoefer, P. P. M. So, D. Thompson, and M. M. Tentzeris, "Topology and design of wide-band 3D metamaterials made of periodically loaded transmission line arrays," *Proc. IEEE MTT-S International Microwave Symposium*, Long Beach, USA, June 12–17, 2005, pp. 313–316.

[100] M. Zedler, C. Caloz, and P. Russer, "A 3-D isotropic left-handed metamaterial based on the rotated transmission-line matrix (TLM) scheme," *IEEE Trans. Microw. Theory Tech.*, vol. 55, no. 12, Pt. 2, pp. 2930–2941, 2007.

[101] A. K. Iyer and G. V. Eleftheriades, "A multilayer negative-refractive-index transmission-line (NRI-TL) metamaterial free-space lens at X-band," *IEEE Trans. Antennas Propag.*, vol. 55, no. 10, pp. 2746–2753, 2007.

[102] S. M. Rudolph and A. Grbic, "Volumetric negative-refractive-index medium exhibiting broadband negative permeability," *J. Appl. Phys.*, vol. 102, no. 1, p. 013904, 2007.

[103] A. K. Iyer and G. V. Eleftheriades, "Mechanisms of subdiffraction free-space imaging using a transmission-line metamaterial superlens: An experimental verification," *Appl. Phys. Lett.*, vol. 92, no. 13, p. 131105, 2008.

[104] J. Zhu and G. V. Eleftheriades, "Experimental verification of overcoming the diffraction limit with a volumetric Veselago–Pendry transmission-line lens," *Phys. Rev. Lett.*, vol. 101, no. 1, p. 013902, 2008.

[105] S. Maslovski and S. Tretyakov, "Phase conjugation and perfect lensing," *J. Appl. Phys.*, vol. 94, no. 7, pp. 4241–4243, 2003.

[106] M. J. Freire and R. Marques, "Planar magnetoinductive lens for three-dimensional subwavelength imaging," *Appl. Phys. Lett.*, vol. 86, no. 18, p. 182505, 2005.

[107] M. J. Freire, R. Marques, and D. Baena, "Three-dimensional superresolution in metamaterial slab lenses: Experiment and theory," *Phys. Rev. B*, vol. 72, no. 23, p. 235117, 2005.

[108] N. Fang, H. Lee, C. Sun, and X. Zhang, "Sub-diffraction-limited optical imaging with a silver superlens," *Science*, vol. 308, no. 5721, pp. 534–537, 2005.

[109] P. A. Belov, C. R. Simovski, and P. Ikonen, "Canalization of subwavelength images by electromagnetic crystals," *Phys. Rev. B*, vol. 71, no. 19, p. 193105, 2005.

[110] P. Ikonen, P. Belov, C. Simovski, and S. Maslovski, "Experimental demonstration of subwavelength field channeling at microwave frequencies using a capacitively loaded wire medium," *Phys. Rev. B*, vol. 73, no. 7, p. 073102, 2006.

[111] P. Ikonen, C. Simovski, S. Tretyakov, P. Belov, and Y. Hao, "Magnification of subwavelength field distributions at microwave frequencies using a wire medium slab operating in the canalization regime," *Appl. Phys. Lett.*, vol. 91, no. 10, p. 104102, 2007.

[112] P. A. Belov, Y. Zhao, S. Tse, P. Ikonen, M. G. Silveirinha, C. R. Simovski, S. Tretyakov, Y. Hao, and C. Parini, "Transmission of images with subwavelength resolution to distances of several wavelengths in the microwave range," *Phys. Rev. B*, vol. 77, no. 19, p. 193108, 2008.

[113] Z. Jacob, L. V. Alekseyev, and E. Narimanov, "Optical hyperlens: Far-field imaging beyond the diffraction limit," *Optics Express*, vol. 14, no. 18, pp. 8247–8256, 2006.

[114] A. Salandrino and N. Engheta, "Far-field subdiffraction optical microscopy using metamaterial crystals: Theory and simulations," *Phys. Rev. B*, vol. 74, no. 7, p. 075103, 2006.

[115] Z. Liu, H. Lee, Y. Xiong, C. Sun, and X. Zhang, "Far-field optical hyperlens magnifying sub-diffraction-limited objects," *Science*, vol. 315, no. 5819, p. 1686, 2007.

[116] A. M. H. Wong, C. D. Sarris and G. V. Eleftheriades, "Metallic transmission screen for sub-wavelength focusing," *Electronics Lett.*, vol. 43, no. 25, pp. 1402–1404, 2007.

[117] G. V. Eleftheriades and A. M. H. Wong, "Holography-inspired screens for sub-wavelength focusing in the near field," *IEEE Microw. Wireless Compon. Lett.*, vol. 18, no. 4, pp. 236–238, 2008.

[118] A. Grbic, L, Jiang, and R. Merlin, "Near-field plates: Subdiffraction focusing with patterned surfaces," *Science*, vol. 320, no. 5874, pp. 511–513, 2008.

[119] A. Grbic and R. Merlin, "Near-field focusing plates and their design," *IEEE Trans. Antennas Propag.*, vol. 56, no. 10, pp. 3159–3165, 2008.

[120] P. Alitalo, L. Jylhä, A. Karttunen, O. Luukkonen, G. Molera, H. Rimminen, M. Vaaja, J. Venermo, V. Podlozny, A. Sihvola, S. Tretyakov, and H. Wallen, "Realization of an electromagnetic invisibility cloak by transmission-line networks," *Proc. Metamaterials'2007*, Rome, Italy, October 22–24, 2007, pp. 953–956.

[121] P. Alitalo and S. Tretyakov, "Cylindrical transmission-line cloak for microwave frequencies," *Proc. IEEE International Workshop on Antenna Technology*, Chiba, Japan, March 4–6, 2008, pp. 147–150.

[122] P. Alitalo and S. Tretyakov, "On electromagnetic cloaking - general principles, problems and recent advances using the transmission-line approach," *Proc. XXIX URSI General Assembly*, Chicago, USA, August 7–16, 2008, p. B01p9.

[123] P. Alitalo and S. Tretyakov, "Broadband microwave cloaking with periodic networks of transmission lines," *Proc. Metamaterials'2008*, Pamplona, Spain, September 21–26, 2008, pp. 392–394.

[124] S. A. Tretyakov, I. S. Nefedov, and P. Alitalo, "Generalized field transformations using metamaterials," *Proc. Metamaterials'2008*, Pamplona, Spain, September 21–26, 2008, pp. 597–599.

[125] S. A. Tretyakov, I. S. Nefedov, and P. Alitalo, "Generalized field-transforming metamaterials," *New J. Phys.*, vol. 10, no. 11, p. 115028, 2008.

[126] P. Alitalo, O. Luukkonen, L. Jylhä, J. Venermo, and S. A. Tretyakov, Correction to "Transmission-line networks cloaking objects from electromagnetic fields," *IEEE Trans. Antennas Propag.*, vol. 56, no. 3, p. 918, 2008.

[127] A. Alù and N. Engheta, "Plasmonic materials in transparency and cloaking problems: Mechanism, robustness, and physical insights," *Optics Express*, vol. 15, no. 6, pp. 3318–3332, 2007.

[128] M. G. Silveirinha, A. Alù, and N. Engheta, "Parallel-plate metamaterials for cloaking structures," *Phys. Rev. E*, vol. 75, no. 3, p. 036603, 2007.

[129] A. Alù and N. Engheta, "Cloaking and transparency for collections of particles with metamaterial and plasmonic covers," *Optics Express*, vol. 15, no. 12, pp. 7578–7590, 2007.

[130] A. Alù and N. Engheta, "Multi-frequency optical invisibility cloaks with layered plasmonic shells," *Phys. Rev. Lett.*, vol. 100, no. 11, p. 113901, 2008.

[131] M. G. Silveirinha, A. Alù, and N. Engheta, "Infrared and optical invisibility cloak with plasmonic implants based on scattering cancellation," *Phys. Rev. B*, vol. 78, no. 7, p. 075107, 2008.

[132] A. Alù and N. Engheta, "Theory and potentials of multi-layered plasmonic covers for multi-frequency cloaking," *New J. Phys.*, vol. 10, no. 11, p. 115036, 2008.

[133] A. Alù and N. Engheta, "Effects of size and frequency dispersion in plasmonic cloaking," *Phys. Rev. E*, vol. 78, no. 4, p. 045602(R), 2008.

[134] F. Bilotti, S. Tricarico, and L. Vegni, "Electromagnetic cloaking devices for TE and TM polarizations," *New J. Phys.*, vol. 10, no. 11, p. 115035, 2008.

[135] D. Schurig, J. J. Mock, B. J. Justice, S. A. Cummer, J. B. Pendry, A. F. Starr, and D. R. Smith, "Metamaterial electromagnetic cloak at microwave frequencies," *Science*, vol. 314, no. 5801, pp. 977–980, 2006.

[136] A. Greenleaf, M. Lassas, and G. Uhlmann, "Anisotropic conductivities that cannot be detected by EIT," *Physiol. Meas.*, vol. 24, pp. 413–420, 2003.

[137] A. Greenleaf, M. Lassas, and G. Uhlmann, "On nonuniqueness for Calderon's inverse problem," *Math. Res. Lett.*, vol. 10, no. 5–6, pp. 685–693, 2003.

[138] L. S. Dollin, "On the possibility of comparison of three-dimensional electromagnetic systems with nonuniform anisotropic filling," *Izv. VUZov Radiofizika*, vol. 4, no. 5, pp. 964–967, 1961 (in Russian).

[139] U. Leonhardt, "Notes on conformal invisibility devices," *New J. Phys.*, vol. 8, no. 7, p. 118, 2006.

[140] U. Leonhardt, "General relativity in electrical engineering," *New J. Phys.*, vol. 8, no. 10, p. 247, 2006.

[141] S. A. Cummer, B. I. Popa, D. Schurig, D. R. Smith, and J. B. Pendry, "Full-wave simulations of electromagnetic cloaking structures," *Phys. Rev. E*, vol. 74, no. 3, p. 036621, 2006.

[142] D. Schurig, J. B. Pendry, and D. R. Smith, "Calculation of material properties and ray tracing in transformation media," *Optics Express*, vol. 14, no. 21, pp. 9794–9804, 2006.

[143] U. Leonhardt, "Optical metamaterials: Invisibility cup," *Nature Photonics*, vol. 1, pp. 207–208, 2007.

[144] A. Greenleaf, Y. Kurylev, M. Lassas, and G. Uhlmann, "Full-wave invisibility of active devices at all frequencies," *Commun. Math. Phys.*, vol. 275, no. 3, pp. 749–789, 2007.

[145] F. Zolla, S. Guenneau, A. Nicolet, and J. B. Pendry, "Electromagnetic analysis of cylindrical invisibility cloaks and the mirage effect," *Optics Lett.*, vol. 32, no. 9, pp. 1069–1071, 2007.

[146] Z. Ruan, M. Yan, C. W. Neff, and M. Qiu, "Ideal cylindrical cloak: Perfect but sensitive to tiny perturbations," *Phys. Rev. Lett.*, vol. 99, no. 11, p. 113903, 2007.

[147] W. Cai, U. K. Chettiar, A. V. Kildishev, and V. M. Shalaev, "Optical cloaking with metamaterials," *Nature Photonics*, vol. 1, pp. 224–227, 2007.

[148] M. Yan, Z. Ruan, and M. Qiu, "Cylindrical invisibility cloak with simplified material parameters is inherently visible," *Phys. Rev. Lett.*, vol. 99, no. 23, p. 233901, 2007.

[149] M. Yan, Z. Ruan, and M. Qiu, "Scattering characteristics of simplified cylindrical invisibility cloaks," *Optics Express*, vol. 15, no. 26, pp. 17772–17782, 2007.

[150] W. Cai, U. K. Chettiar, A. V. Kildishev, V. M. Shalaev, and G. W. Milton, "Nonmagnetic cloak with minimized scattering," *Appl. Phys. Lett.*, vol. 91, no. 11, p. 111105, 2007.

[151] H. Chen, B.-I. Wu, B. Zhang, and J. A. Kong, "Electromagnetic wave interactions with a metamaterial cloak," *Phys. Rev. Lett.*, vol. 99, no. 6, p. 063903, 2007.

[152] H. Chen, Z. Liang, P. Yao, X. Jiang, H. Ma, and C. T. Chan, "Extending the bandwidth of electromagnetic cloaks," *Phys. Rev. B*, vol. 76, no. 24, p. 241104(R), 2007.

[153] K. Guven, E. Saenz, R. Gonzalo, E. Ozbay and S. A. Tretyakov, "Electromagnetic cloaking with canonical spiral inclusions," *New J. Phys.*, vol. 10, no. 11, p. 115037, 2008.

[154] W. Cai, U. K. Chettiar, A. V. Kildishev, and V. M. Shalaev, "Designs for optical cloaking with high-order transformations," *Optics Express*, vol. 16, no. 8, pp. 5444–5452, 2008.

[155] D. P. Gaillot, C. Croenne, F. Zhang, and D. Lippens, "Transformation optics for the full dielectric electromagnetic cloak and metal-dielectric planar hyperlens," *New J. Phys.*, vol. 10, no. 11, p. 115039, 2008.

[156] A. V. Kildishev, W. Cai, U. K. Chettiar, and V. M. Shalaev, "Transformation optics: Approaching broadband electromagnetic cloaking," *New J. Phys.*, vol. 10, no. 11, p. 115029, 2008.

[157] A. D. Yaghjian and S. Maci, "Alternative derivation of electromagnetic cloaks and concentrators," *New J. Phys.*, vol. 10, no. 11, p. 115022, 2008.

[158] I. I. Smolyaninov, "Transformational optics of plasmonic metamaterials," *New J. Phys.*, vol. 10, no. 11, p. 115033, 2008.

[159] A. Greenleaf, Y. Kurylev, M. Lassas, and G. Uhlmann, "Isotropic transformation optics: Approximate acoustic and quantum cloaking," *New J. Phys.*, vol. 10, no. 11, p. 115024, 2008.

[160] S. A. Cummer, M. Rahm, and D. Schurig, "Material parameters and vector scaling in transformation acoustics," *New J. Phys.*, vol. 10, no. 11, p. 115025, 2008.

[161] J. Li and J. B. Pendry, "Hiding under the carpet: A new strategy for cloaking," *Phys. Rev. Lett.*, vol. 101, no. 20, p. 203901, 2008.

[162] P. Yao, Z. Liang, and X. Jiang, "Limitation of the electromagnetic cloak with dispersive material," *Appl. Phys. Lett.*, vol. 92, no. 3, p. 031111, 2008.

[163] B. Zhang, B.-I. Wu, H. Chen, and J. A. Kong, "Rainbow and blueshift effect of a dispersive spherical invisibility cloak impinged on by a nonmonochromatic plane wave," *Phys. Rev. Lett.*, vol. 101, no. 6, p. 063902, 2008.

[164] S. A. Cummer, B.-I. Popa, D. Schurig, D. R. Smith, J. Pendry, M. Rahm, and A. Starr, "Scattering theory derivation of a 3D acoustic cloaking shell," *Phys. Rev. Lett.*, vol. 100, no. 2, p. 024301, 2008.

[165] M. Farhat, S. Enoch, S. Guenneau, and A. B. Movchan, "Broadband cylindrical acoustic cloak for linear surface waves in a fluid," *Phys. Rev. Lett.*, vol. 101, no. 13, p. 134501, 2008.

[166] D.-H. Kwon and D. H. Werner, "Two-dimensional eccentric elliptic electromagnetic cloaks," *Appl. Phys. Lett.*, vol. 92, no. 1, p. 013505, 2008.

[167] W. X. Jiang, J. Y. Chin, Z. Li, Q. Chen, R. Liu, and T. J. Cui, "Analytical design of conformally invisible cloaks for arbitrarily shaped objects," *Phys. Rev. E*, vol. 77, no. 6, p. 066607, 2008.

[168] Y. Zhao, C. Argyropoulos, and Y. Hao, "Full-wave finite-difference time-domain simulation of electromagnetic cloaking structures," *Optics Express*, vol. 16, no. 9, pp. 6717–6730, 2008.

[169] W. Yan, M. Yan, Z. Ruan, and M. Qiu, "Influence of geometrical perturbation at inner boundaries of invisibility cloaks," *J. Opt. Soc. Am. A*, vol. 25, no. 4, pp. 968–973, 2008.

[170] W. Yan, M. Yan, Z. Ruan, and M. Qiu, "Coordinate transformation makes perfect invisibility cloaks with arbitrary shape," *New J. Phys.*, vol. 10, no. 4, p. 043040, 2008.

[171] L. Zhang, M. Yan, and M. Qiu, "The effect of transformation order on the invisibility performance of a practical cylindrical cloak," *J. Opt. A*, vol. 10, p. 095001, 2008.

[172] W. Yan, M. Yan, and M. Qiu, "Non-magnetic simplified cylindrical cloak with suppressed zeroth order scattering," *Appl. Phys. Lett.*, vol. 93, no. 2, p. 021909, 2008.

[173] P. Collins and J. McGuirk, "A novel methodology for deriving improved material parameter sets for simplified cylindrical cloaks," *J. Opt. A*, vol. 11, p. 015104, 2009.

[174] R. Liu, C. Ji, J. J. Mock, J. Y. Chin, T. J. Cui, and D. R. Smith, "Broadband ground-plane cloak," *Science*, vol. 323, no. 5912, pp. 366–369, 2009.

[175] P.-S. Kildal, A. A. Kishk, and A. Tengs, "Reduction of forward scattering from cylindrical objects using hard surfaces," *IEEE Trans. Antennas Propag.*, vol. 44, no. 11, pp. 1509–1520, 1996.

[176] P.-S. Kildal, A. Kishk, and Z. Sipus, "RF invisibility using metamaterials: Harry Potter's cloak or the emperor's new clothes?" *Proc. IEEE International Symposium on Antennas and Propagation*, Honolulu, USA, June 10–15, 2007, pp. 2361–2364.

[177] G. W. Milton and N.-A. P. Nicorovici, "On the cloaking effects associated with anomalous localized resonance," *Proc. R. Soc. Lond. A: Math. Phys. Sci.*, vol. 462, pp. 3027–3059, 2006.

[178] N.-A. P. Nicorovici, G. W. Milton, R. C. McPhedran, and L. C. Botten, "Quasistatic cloaking of two-dimensional polarizable discrete systems by anomalous resonance," *Optics Express*, vol. 15, no. 10, pp. 6314–6323, 2007.

[179] N.-A. P. Nicorovici, R. C. McPhedran, S. Enoch, and G. Tayeb, "Finite wavelength cloaking by plasmonic resonance," *New J. Phys.*, vol. 10, no. 11, p. 115020, 2008.

[180] P. Alitalo, O. Luukkonen, and S. A. Tretyakov, "Wide-band electromagnetic cloaking with a simple volumetric structure composed of metal plates," *Proc. Metamaterials'2009*, London, UK, August 30–September 4, 2009, in press.

[181] P. M. T. Ikonen, P. Alitalo, and S. A. Tretyakov, "On impedance bandwidth of resonant patch antennas implemented using structures with engineered dispersion," *IEEE Antennas Wireless Propag. Lett.*, vol. 6, pp. 186–190, 2007.

[182] P. Ikonen, P. Alitalo, and S. Tretyakov, "Loaded transmission-line meshes as artificial materials for some antenna applications," *Proc. 23rd Annual Review of Progress in Applied Computational Electromagnetics*, Verona, Italy, March 19–23, 2007, pp. 135–138.

[183] P. Alitalo, J. Vehmas, O. Luukkonen, L. Jylhä, and S. Tretyakov, "Microwave transmission-line lens matched with free space," *Proc. IEEE International Workshop on Antenna Technology*, Chiba, Japan, March 4–6, 2008, pp. 282–285.

[184] Y. T. Lo and S. W. Lee, Eds., *Antenna handbook: Theory applications and design*, New York: Van Nostrand Reinhold, 1988, Chapter 16.

[185] S. Silver, Ed., *Microwave antenna theory and design*, New York: McGraw-Hill, 1949, Chapter 11.

[186] H. Jasik, Ed., *Antenna engineering handbook*, New York: McGraw-Hill, 1961, Chapter 14.

[187] R. E. Collin and F. J. Zucker, Eds., *Antenna theory, Part 2*, New York: McGraw-Hill, 1969, Chapter 18.

[188] S. Cornbleet, *Microwave optics*, New York: Academic Press, 1976.

[189] W. Rotman, "Plasma simulation by artificial dielectrics and parallel-plate media," *IRE Trans. Antennas Propag.*, vol. 10, no. 1, pp. 82–95, 1962.

[190] W. Rotman and R. F. Turner, "Wide-angle microwave lens for line source applications," *IEEE Trans. Antennas Propag.*, vol. 11, no. 6, pp. 623–632, 1963.